

JOHN HOLMES

SANDIA REPORT

SAND81-1562 • Unlimited Release • UC-62

Printed September 1981

A User's Guide to HELIOS: A Computer Program for Modeling the Optical Behavior of Reflecting Solar Concentrators

Charles N. Vittitoe, Frank Biggs

Prepared by
Sandia National Laboratories
Albuquerque, New Mexico 87185 and Livermore, California 94550
for the United States Department of Energy
under Contract DE-AC04-76DP00789



SF2900Q(8-81)

Issued by Sandia National Laboratories, operated for the United States Department of Energy by Sandia Corporation.

NOTICE: This report was prepared as an account of work sponsored by an agency of the United States Government. Neither the United States Government nor any agency thereof, nor any of their employees, nor any of their contractors, subcontractors, or their employees, makes any warranty, express or implied, or assumes any legal liability or responsibility for the accuracy, completeness, or usefulness of any information, apparatus, product, or process disclosed, or represents that its use would not infringe privately owned rights. Reference herein to any specific commercial product, process, or service by trade name, trademark, manufacturer, or otherwise, does not necessarily constitute or imply its endorsement, recommendation, or favoring by the United States Government, any agency thereof or any of their contractors or subcontractors. The views and opinions expressed herein do not necessarily state or reflect those of the United States Government, any agency thereof or any of their contractors or subcontractors.

Printed in the United States of America
Available from
National Technical Information Service
U.S. Department of Commerce
5285 Port Royal Road
Springfield, VA 22161

NTIS price codes
Printed copy: \$8.00
Microfiche copy: A01

SAND81-1562
Unlimited Release
Printed September 1981

Distribution
Category UC-62

A USER'S GUIDE TO HELIOS: A COMPUTER PROGRAM FOR MODELING
THE OPTICAL BEHAVIOR OF REFLECTING SOLAR CONCENTRATORS

Part III: Appendices Concerning HELIOS--Code Details

Charles N. Vittitoe
Frank Biggs
Theoretical Division 4231
Sandia National Laboratories
Albuquerque, NM 87185

ABSTRACT

HELIOS is a flexible computer code for evaluating designs for central-receiver, parabolic-dish, and other reflecting solar-energy collector systems; for safety calculations on the threat to personnel and to the facility itself; for determination of how various input parameters alter the power collected; for design trade-offs; and for heliostat evaluations. Input variables include atmospheric transmission effects; reflector shape, surface, and suntracking errors; focusing and alignment strategies; receiver design; placement positions of the tower and mirrors; time-of-day and day-of-year for the calculation. Part III is a series of appendices giving code details for sub-routine and function descriptions, how common blocks are used, sample jobstreams, and magnetic tape use within the code.

PREFACE

The user's guide has been divided into a series of parts to reflect its anticipated use. Part I, which is expected to receive the most use, concentrates upon the input. Part II focuses on the output for several sample problems and is useful mainly for learning details that will become automatic after several actual uses of the code. Part III is a series of appendices giving code details such as subroutine and function descriptions, how the common blocks are used, and sample jobstreams. This portion may be useful when code alterations are required to model more exotic collection systems. Other parts describe the plotting and data editing codes and how alterations may be made to treat special heliostat or receiver shapes not available as regular options in HELIOS. Part I includes acknowledgments and notes on code availability and caution that are not repeated here.

CONTENTS

	<u>Page</u>
Introduction	9
APPENDIX A -- Subroutines and Functions	11
APPENDIX B -- Input Variables	53
APPENDIX C -- HELIOS Common-Block Connections	59
APPENDIX D -- HELIOS Common-Block Parameter Lists	63
APPENDIX E -- HELIOS Subroutine Connections	77
APPENDIX F -- File Names in HELIOS	83
APPENDIX G -- Jobstream Examples	85
APPENDIX H -- HELIOS Code Summary	89
References	92

ILLUSTRATIONS

<u>Figure</u>		
A-1	Geometry for Intersection in Aperture Plane	13
A-2	CPQR Subroutine Flow Chart	17
A-3	Declination of the Sun	18
A-4	Flow Diagram for FACET Function	20
A-5	Flow Diagram for OVER	39
A-6	Flow Chart for PHI	40
A-7	Flow Diagram for USERVN	50

TABLES

<u>Table</u>		
A-1	Tape 1 Data From NASTRAN	27
A-2	Facet Normals Before and After Calls to GLOAD for One McDonnell-Douglas Heliostat Design	33

A USER'S GUIDE TO HELIOS: A COMPUTER PROGRAM FOR MODELING
THE OPTICAL BEHAVIOR OF REFLECTING SOLAR CONCENTRATORS

Introduction

Computer-code documentation is complete only when provided for software maintenance, for the code user, and for the analyst. Complete documentation and readily understood and used documentation are often conflicting requirements. Although most users will have little interest in the code structure and internal details, a few will want to make alterations to expand capabilities or treat specific problems. These analysts usually know from experience that changing one portion of a complicated code can have undesired effects on other portions. The series of appendices presented here indicate the interconnections within HELIOS and should reduce the undesired effects.

Appendix A lists the subroutines and functions, along with a brief explanation of their purpose. Some of these are accompanied by flow diagrams and more detailed discussion when the approach is not explained elsewhere. In the Subroutine GLOAD section, for example, directions are given for preparing Tape 1 when gravity- or wind-loading effects are to be included. The input variables are listed alphabetically in Appendix B, along with routines where they are used. Appendix C lists the routines that use each common block; a change in one may require changes in all. Parameters within each common block are defined in Appendix D. Appendix E lists the routines called by and within each subroutine or function. The file names are listed in Appendix F, along with their purposes and where they are used. Appendix G discusses sample jobstreams for computers at Sandia National Laboratories, Albuquerque (SNLA). Although not directly applicable to other users, they serve as a start for processing at other installations. The final appendix (Appendix H) briefly summarizes the HELIOS Code and indicates computer hardware and software requirements. Although these appendices may prove to be dry reading, at least part of them will be valuable for changes or for a better understanding of how certain routines accomplish their mission.

APPENDIX A
Subroutines and Functions

Descriptions are given here for each subroutine and function in HELIOS. The simple routines are described briefly; others, especially those a user is more likely to inquire about or want to change, are investigated in greater detail. The routines are listed alphabetically with discussion following each heading. Standard FORTRAN library functions such as sine, cosine, and arctangent are not listed.

ABSA(A) calculates the absolute value of the vector, A, appearing as the single argument. It is called by APERT, APERTV, C, CONVU, GETNSF, GLOAD, INDATA, ORTAR, PHI, PHID, ROTAT, SHBL, TARGET, and TCIRP.

ABSORP(C) determines the absorptance of the target surface. The single argument, C, is the cosine of the angle of incidence at the target. The absorptance is set to 1.0. In several applications, this function has been altered by users to account for angular variation. The function is called by PHI.

ACRSB(A,B,C) returns in the three-component vector C the cross product of input vectors A and B. The subroutine is called by APERTV, CONVU, GETNSF, GLOAD, and PHI.

ADOTB(A,B) calculates the inner product of two vectors, A and B. The function is called by APERT, APERTV, C, CONVU, FVOT, PHI, PHID, TARGET, and TCIRP.

AIM(XAIM,YAIM,ZAIM) sets the tower coordinates of the proper aim point. The coordinates are returned as the arguments of the subroutine. It is called by TARGET.

ANGL(Y,X) finds the arctangent (Y/X). The function uses the library routine ATAN2 (Y,X) except when $|x| = 0$ (which would result in a fatal error in some libraries). In ANGL when $|x| = 0$, the angle is set to $\pi/2$ ($-\pi/2$) for $Y \geq (<)$ zero. The function is called by AZELA, AZELB, C, CPQR, ELAZS, JITTER, and SHBL.

APADJ(NHELI,HE,HN,HZ,X,Y,Z) sets the tower coordinates (x,y,z) of the aim point for a heliostat with base coordinates HE,HN,HZ and heliostat number NHELI. The routine is used only when INELD=2, where heliostat coordinates are read from Tape 3. The present form is appropriate only for the main receiver of a 100-MWe advanced water/steam receiver system designed by Black and Veatch. The subroutine is called by A and by FPADJ.

APERT(MAPT,XTA,YTA,ZTA,VFE) determines if the cone-optics ray is excluded (MAPT=0) or included (MAPT=1) by the aperture to the target. The tower coordinates of

the elemental area of integration on the facet are given by the vector VFE. The individual target point being considered has tower coordinates XTA, YTA, ZTA. The subroutine is called by FACET.

Optimizing receiver design in a solar-energy collecting system requires taking into account the heat radiated from a receiver that may be at temperatures >1000°C. One way of reducing this energy loss is to use a cavity receiver to decrease the effective high-temperature area that radiates to the surroundings (as well as to reduce convection loss). This approach requires the solar energy to pass through an aperture before collection by the enclosed heat exchanger. Here we describe the method HELIOS uses to test its cone-optics rays for passage through an aperture defined by coordinates of four points that lie in a plane. In several applications the method has been altered to account for up to five separate apertures.

Let us first assume that the aperture is a rectangle with tower coordinates of the four aperture corners given by input variables (AC(I,J), J=1,3) for corners I=1 through 4. The corners are assumed labeled clockwise from the upper left corner as seen by a photon entering the aperture. The aperture is assumed to have two horizontal edges. Vectors from corner 1 to 2 and from corner 4 to 1 are given by V₁₂ and V₄₁ with components

$$V_{12}(I) = AC(2,I) - AC(1,I), I=1,3 \quad ,$$

$$V_{41}(I) = AC(1,I) - AC(4,I), I=1,3 \quad .$$

The corresponding unit vectors are designated u₁₂ and u₄₁. The horizontal dimension of the aperture is |V₁₂| (=2.*HXL). The length of the other edges of the aperture is |V₄₁| (=2.*HYL). These variables are calculated in INDATA when the aperture option is exercised. In Subroutine FACET, the call to VECCT gives the tower coordinates of the integration-element center (VFE(I), I=1,3).

A vector from the integration-element center to the target point has coordinates

$$\underline{ECT} = (XTA-VFE(1), YTA-VFE(2), ZTA-VFE(3)) \quad ,$$

with corresponding unit vector $\underline{UECT} = \frac{\underline{ECT}}{|\underline{ECT}|}$. Let the distance along UECT from the element center to the aperture plane be given by d. Then

$$d \underline{UECT} = \underline{V}_1 + \alpha \underline{V}_{12} + \beta \underline{V}_{41} \quad ,$$

where V₁ has components (AC(1,I)-VFE(I), I=1,3). The three components give three equations in the three unknowns d, α, and β. Solving for d by determinants gives

$$d = \frac{\begin{vmatrix} V_1(1) & V_{12}(1) & V_{41}(1) \\ V_1(2) & V_{12}(2) & V_{41}(2) \\ V_1(3) & V_{12}(3) & V_{41}(3) \end{vmatrix}}{\begin{vmatrix} U_1 & V_{12}(1) & V_{41}(1) \\ U_2 & V_{12}(2) & V_{41}(2) \\ U_3 & V_{12}(3) & V_{41}(3) \end{vmatrix}}$$

In the tower-coordinate system, the components of a vector from the integration element along UECT to the aperture plane is d UECT. Coordinates in the aperture plane are given by

$$AIP(I) = d \text{ UECT}(I) - V_c(I)$$

where $V_c(I)$ are coordinates of the aperture center. The components $AIP(I)$ are measured in a coordinate system with origin at the aperture center and with its axes parallel to the tower coordinate axes. The center is given by

$$V_c(I) = V_1(I) + 0.5 V_{12}(I) - 0.5 V_{41}(I)$$

Figure A-1 illustrates the geometry.

We now construct an aperture coordinate system with x-axis horizontal and y-axis orthogonal to x in the aperture plane. In this system, the coordinates of the intersection point are

$$x_{ap} = \underline{AIP} \cdot \underline{U}_{12}$$

$$y_{ap} = \underline{AIP} \cdot \underline{U}_{41}$$

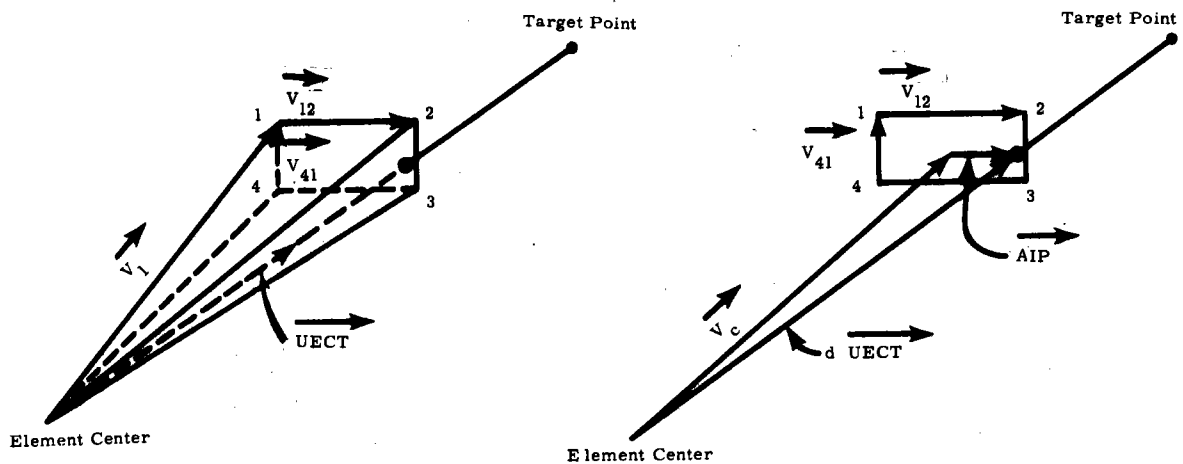


Figure A-1. Geometry for Intersection in Aperture Plane

The ray successfully traverses the aperture only when

$$|x_{ap}| < \frac{|V_{12}|}{2} \equiv HXL$$

and

$$|y_{ap}| < \frac{|V_{41}|}{2} \equiv HYL$$

Let us now assume the aperture is circular. Mathematically we construct a square inscribed inside the boundary. Let two sides of the square be horizontal. The tower coordinates of the corners of this square are now assigned as the values (AC(I,J),J=1,3) for the four corners I=1 through 4. The labeling order is as for the rectangular case. The square fixes the aperture radius and its orientation in space. Keeping the notation introduced earlier, we find that the ray successfully traverses the circular aperture when

$$x_{ap}^2 + y_{ap}^2 \leq HXL^2 + HYL^2$$

The aperture option is assigned to the receiver-data group, NGRUP=3. Input variable IAPT determines the type of aperture treated. At present the third corner AC(3,J),J=1,3 is not used because the other corners completely define the aperture and its orientation. However, future generalizations may need to specify an additional corner.

APERTV(MAPT,ECT,UECT,V1,VFE), a special-purpose subroutine, tests 20 points along a cone-optics ray for entering a three-dimensional body of revolution. The subroutine is called by APERT when IAPT=3. It is included in the code as an example of how to treat blocking by a three-dimensional object. A later part of the user's guide describes how APERT is altered and how APERTV is used in a special case.

ATM(ZETA,IND) calculates the atmospheric mass (ATMA) traversed by the sun's rays as a function of the apparent elevation angle (ZETA) of the sun. Data statements give the atmospheric mass (VMASS(I),I=1,295) for a series of apparent elevation angles (ELV(I),I=1,295). Linear interpolation is used between the tabulated values. The first call (IND=1) specifies the ELV values. This subroutine is called by DATA1(IND=1) and by ELAZS(IND=0).

AUTSUN specifies the sunshape parameters for a single-gaussian distribution with an rms width consistent with the value of solar insolation. The rms width is given by

$$\delta = \frac{3.7648 - 0.0038413(I-1000.) + 1.5923E-5(I-1000.)^2}{1000.}$$

where I is in W/m². The rms width of the effective sunshape is

$$R = [\delta^2 + \text{EPSV}^2]$$

The cutoff value of the effective sunshape is set to $\text{BLIM}=3 R$. Because of the cutoff the normalization factor is

$$\text{ZNORM} = \frac{1}{1. - \exp(-\text{BLIM}^2/R^2)}$$

and the dispersion (σ) of the gaussian effective sunshape

$$f(\rho) = \frac{\text{ZNORM} * e^{-\rho^2/2\sigma^2}}{2\pi\sigma^2}$$

is defined by

$$\sigma^2 = R^2/2$$

This subroutine is used with the choices $\text{JSUN}=8$ and $\text{ICON}=0$ or 3 and is called by HELIOS.

AZELA(N) gives the azimuthal and elevation angles for the aim point and the heliostat. $N=0$ gives approximate values. $N=1$ provides the iteration required for convergence to the actual values. The routine is called by Program A; hence the values apply to the orientation defined by the canting geometry.

AZELB(N) calculates the azimuthal and elevation angles for the aim point and the heliostat. It is similar to AZELA. The main difference is its call by Program B; so the values apply to the actual calculation times rather than the prealignment (canting) time. N values 0 and 1 are as for AZELA. N values 2 or 4 result in obtaining the angles by slueing from previous values. These N values correspond to NTLOCK values 2 or 4 . The subroutine may also call JITTER (if JITT.NE.0), which will alter the angles slightly, consistent with the encoder least-count.

BASKET(XI,YI,ZI,IBASX,IBASY), used with reconcentrators, tabulates that portion of the target which receives the cone-optics ray reflected from the reconcentrator. Values of IBASX and IBASY from 1 to 11 correspond to the 11×11 array of usual target points. Parameters XI,YI,ZI are the tower coordinates of the reflected-ray intersection with the target plane. The subroutine is called by FACET and is set up for the example reconcentrator described in Section 8.1.2 of Reference 1. Other reconcentrators require alteration of the routine.

CONE(TANAL) calculates the sunshape, error cone, or effective sunshape for given $\text{TANAL} = \rho = \tan \alpha$. It is called by FFONE for sunshape evaluation and by PHI for effective sunshape evaluation when $\text{ICON} \leq 3$.

CONEA(TANAL) functions effectively the same as CONE. It is called by D for printout of the sunshape, error cone, and effective sunshape. The routine is called by FF and GG for other evaluations of the sunshape and error cone, respectively. It is called by TONE as an aid in normalizing the two-dimensional probability-density functions to unit integral.

CONV provides the convolution of two probability-density functions. Fast-Fourier transforms are used. The subroutine is called by Program D and is used when ICON=1.

CONVU converts the VTAR input vectors that specify a rectangular target plane into a set of unit vectors (1) horizontal, (2) along the orthogonal dimension in the target plane, and (3) orthogonal to the target surface. The subroutine is called DATA1 and by INDATA.

COORD(VTAR11,VTAR23,VTAR,IXPTS,IYPTS,MIDC,DX,MIDR,DZ,XM,YM,ITARSH) uses input values of VTAR(I,J), ITARSH, IXPTS, IYPTS, MIDC, DX, MIDR, DZ to determine the matrices XM(I), YM(I) that are coordinate labels for the output of the flux-density matrices. A user who defines his own target shape (ITARSH=2) may also wish to alter COORD for convenient labeling. The subroutine is called by Program C.

CPQR calculates the unit vectors (PN, QN, RN) for each facet at the time of canting and focusing for later use in NORF. If facet shape is to be determined, this subroutine also calculates the focal length, radius of curvature; or, in the case of a shape determined by stress analysis, the routine calculates the pulldown distance that maximizes the flux density at the prealignment point. This subroutine is called by Program A. Figure A-2 gives the flow chart.

CSHAPE(ECARR, ECXRR, ECYRR, U, V) calculates the amplitude of the effective sunshape at coordinates U, V in the reflected-ray coordinate system as a function of the elliptic-normal error cone (described by parameters ECARR, ECXRR, ECYRR) and a sunshape represented as a sum of gaussian distributions. The function is called by PHI when IANLYT \geq 2 and ICON > 3.

DATA1 sets default values for most input variables and for several mathematical constants. DATA1 is called by A.

DECSUN(D) calculates the declination of the sun as a function of the day-of-year (D). This function is called by HELIOS and by A. The initial functional form used is discussed in Reference 1, pp 27-29. Now we define

$$\phi_0 = \frac{2\pi(D + 284 \text{ days})}{365.24 \text{ days}}$$

as the azimuthal angle of the sun measured in the ecliptic plane in the approximation of a circular orbit for the earth about the sun. The angle is now measured from the sun's position on the 79th day of the year (i.e., March 20 barring leap year, near the vernal equinox). The D is measured in solar

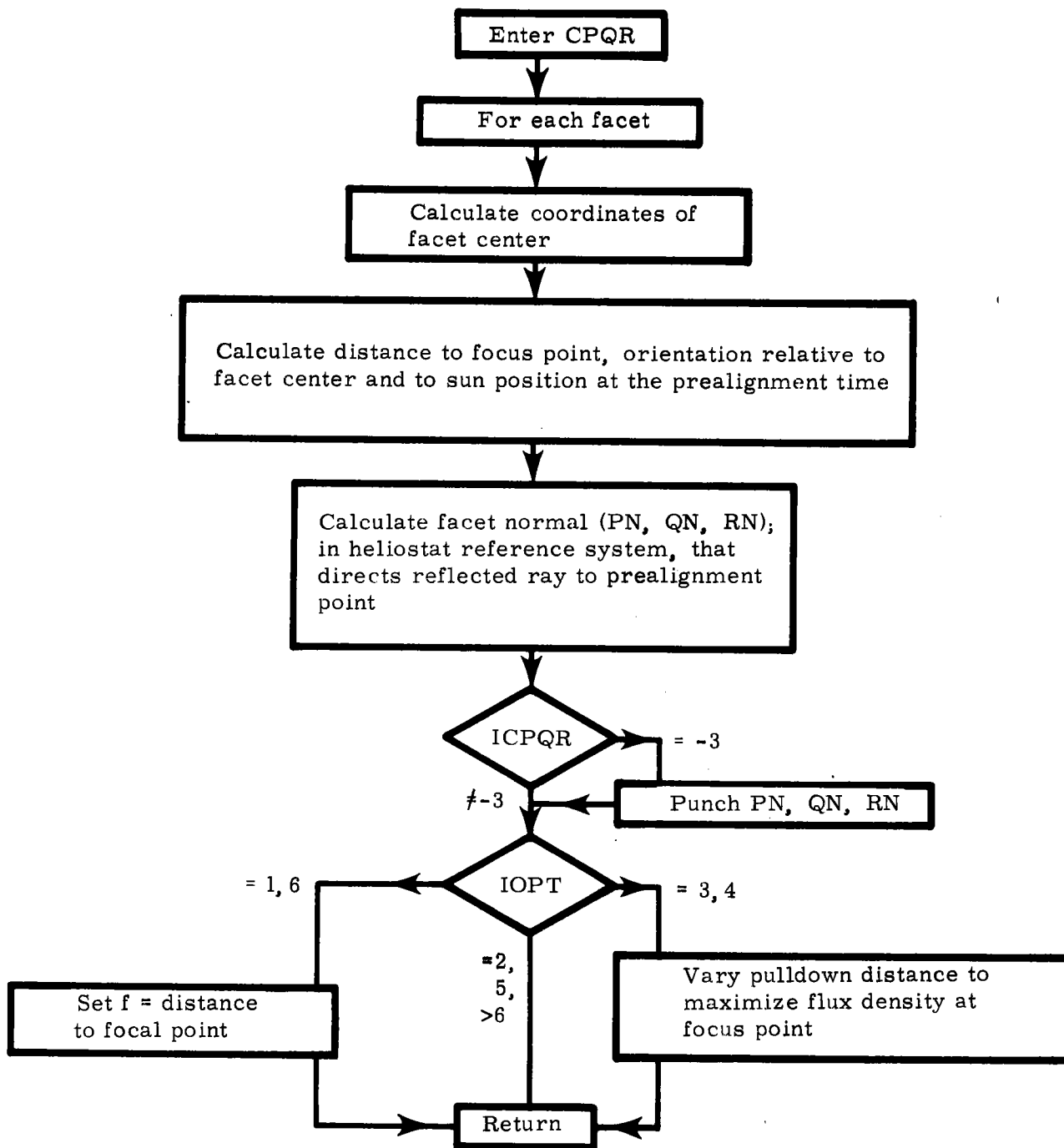


Figure A-2. CPQR Subroutine Flow Chart

days. The improvement in this azimuthal angle occurs because of correction terms to account for the noncircular orbit. Now the azimuthal angle is given by

$$\begin{aligned} \phi_{se}(\text{rad}) = & \phi_0 + 0.007133 \sin \phi_0 + 0.032680 \cos \phi_0 - 0.000318 \sin 2\phi_0 \\ & + 0.000145 \cos 2\phi_0 \end{aligned}$$

This form has been used by M. Collares-Pereira and A. Rabl.² The form is reported to have greater accuracy.

As before, the declination is found from

$$\sin \delta_s = \sin \delta_0 \sin \phi_{se}$$

where $\delta_0 = 23^\circ.442274$. The declination is plotted in Figure A-3. The δ_s is zero for $D = 79.3453$.

ELAZS calculates the azimuthal angle for the sun, its apparent elevation angle, the atmospheric mass traversed by the sun's rays, and the solar insolation (to be used if INSOL.NE.2). The subroutine is called by Program A and by HELIOS.

ELNOR($\sigma_x, \sigma_y, \theta, \sigma_u, \sigma_v, \eta, \sigma_t, \sigma_w$) convolves the input elliptic normal probability-density functions

$$f(x,y) = \frac{1}{2\pi\sigma_x\sigma_y} \exp \left[-\frac{x^2}{2\sigma_x^2} - \frac{y^2}{2\sigma_y^2} \right]$$

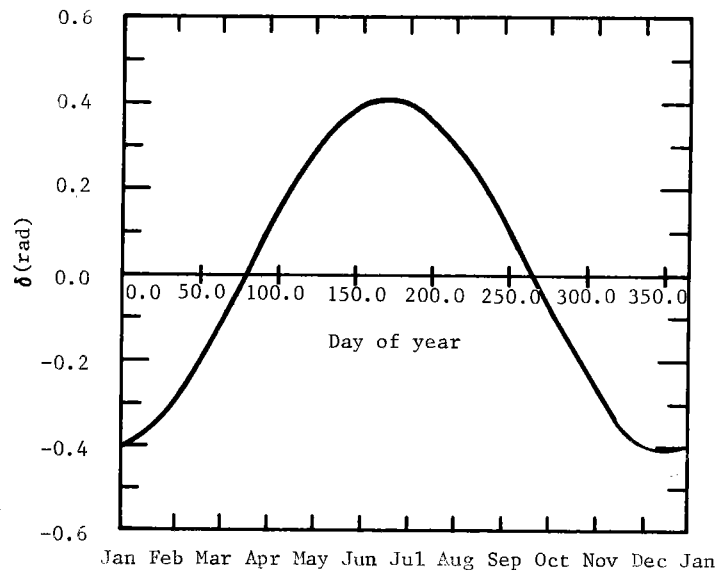


Figure A-3. Declination of the Sun

and

$$g(u, v) = \frac{1}{2\pi\sigma_u\sigma_v} \exp \left[-\frac{u^2}{2\sigma_u^2} - \frac{v^2}{2\sigma_v^2} \right]$$

where the x,y axes rotated by θ degrees give the u,v axes. The convolution (output) is

$$h(t, w) = \frac{1}{2\pi\sigma_t\sigma_w} \exp \left[-\frac{t^2}{2\sigma_t^2} - \frac{w^2}{2\sigma_w^2} \right]$$

η is the angle (in degrees) from the x-axis to the t-axis. The convolution is discussed in Appendix C of Reference 1. This subroutine is called by Subroutine PHI and by INDATA.

ELROT(x,y,sin θ ,cos θ , σ_x , σ_y) evaluates the elliptic-normal probability-density function

$$ELROT = \frac{1}{2\pi\sigma_x\sigma_y} \exp \left[-\frac{u^2}{2\sigma_x^2} - \frac{v^2}{2\sigma_y^2} \right]$$

where the u,v axes are rotated by θ with respect to the x,y axes.

$$\begin{pmatrix} u \\ v \end{pmatrix} = \begin{pmatrix} \cos \theta & \sin \theta \\ -\sin \theta & \cos \theta \end{pmatrix} \begin{pmatrix} x \\ y \end{pmatrix}$$

This function is called by NUCONV and by PHI.

ENORM(σ_1 , σ_2 , θ ,cos i , η_1 , η_2 , β) transforms an elliptic-normal probability-density function from its concentrator reference plane (P-Q) into its reflected-ray reference plane (U-V). In the concentrator plane, the function

$$f_i = \frac{1}{2\pi\sigma_1\sigma_2} \exp \left[-\frac{x^2}{2\sigma_1^2} - \frac{y^2}{2\sigma_2^2} \right]$$

where

$$\begin{pmatrix} x \\ y \end{pmatrix} = \begin{pmatrix} \cos \theta & \sin \theta \\ -\sin \theta & \cos \theta \end{pmatrix} \begin{pmatrix} p \\ q \end{pmatrix}$$

identifies the input variables (Eqs 5.4.8 through 5.4.10 in Reference 1).

The output variables are identified by the function after mapping onto the u-v plane.

$$f_o = \frac{1}{2\pi\eta_1\eta_2} \exp \left[-\frac{s^2}{2\eta_1^2} - \frac{t^2}{2\eta_2^2} \right]$$

where

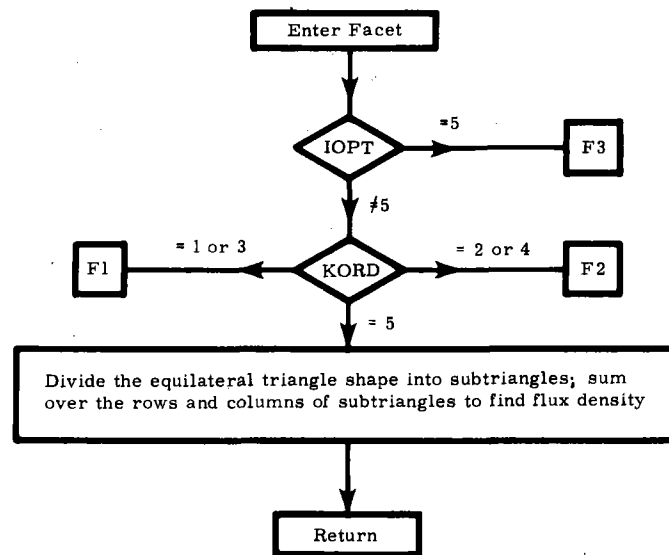
$$\begin{pmatrix} s \\ t \end{pmatrix} = \begin{pmatrix} \cos \beta & \sin \beta \\ -\sin \beta & \cos \beta \end{pmatrix} \begin{pmatrix} u \\ v \end{pmatrix} .$$

The β exits in degrees. The method is described in Reference 1, Section 5.4.2. This subroutine is called by PHI.

ERF(X), a mathematical library function, evaluates the error function of X. It is called by PHI and is listed here because all computer installations may not include ERF in their libraries.

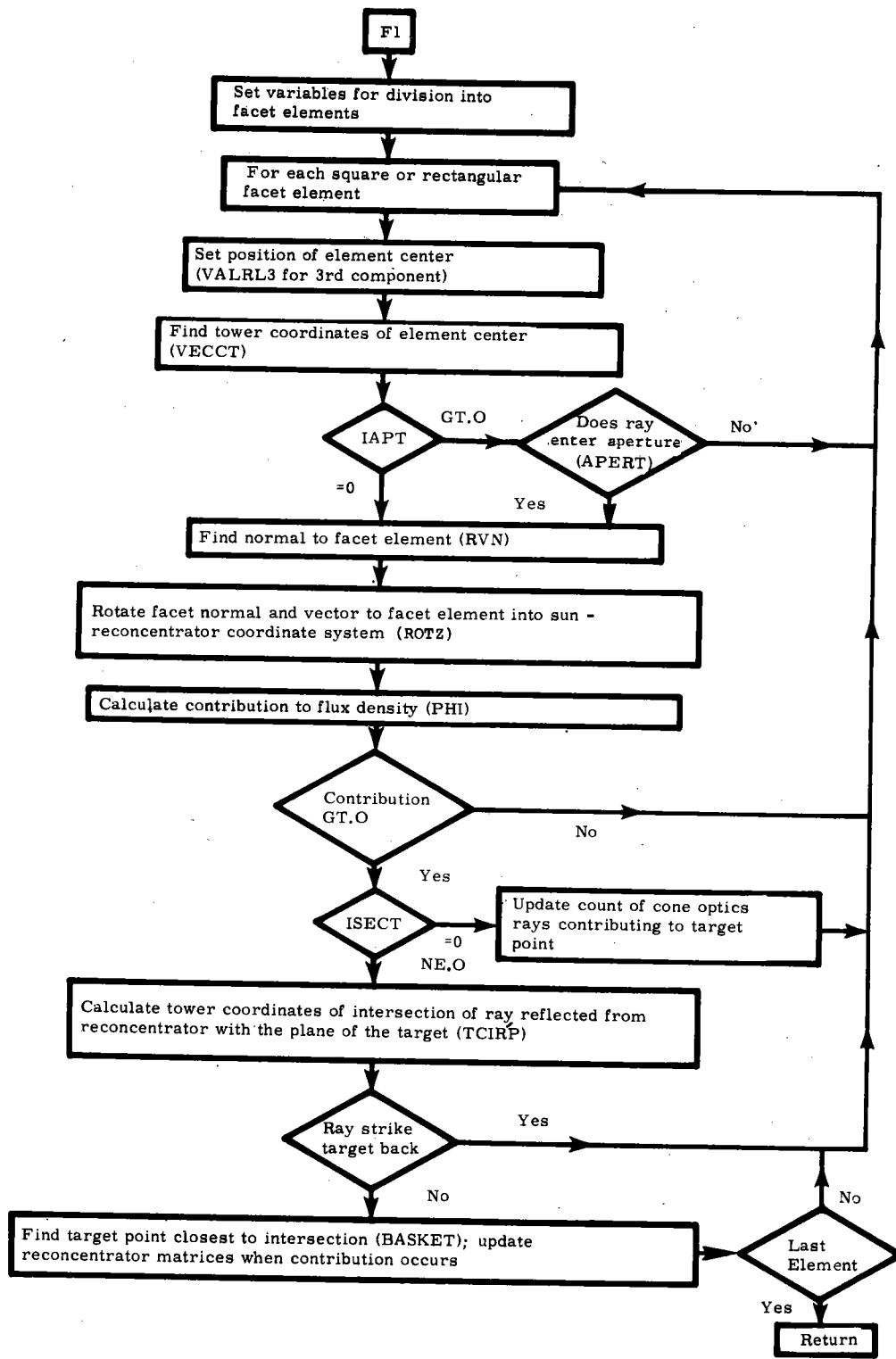
ERRCHK,ERRGET,ERRPRT,ERSTGT,ERXSET together provide a uniform method for processing diagnostics and warning messages that originate in the Sandia National Laboratories (SNL) mathematical program library routines. These subroutines are called by FOURT,GAUS8,MINA,QNC7,RFBS,RULD,SAXB,VAL2D, or by each other. The library is discussed in Reference 3. These library routines have been included in the HELIOS Code itself to try to make the computer code more transferable.

FACET(RB,VM) calculates the flux density (W/cm^2) on an individual target point contributed by one facet for unit reflection coefficient and unit solar insolation. The function is called by Program C. VM is the unit normal at the target point. RB is the vector to the target point in the sun-facet coordinate system. This routine must be altered whenever new facet shapes (outer edges not surface shape) are encountered. See Figure A-4 for the flow diagram.



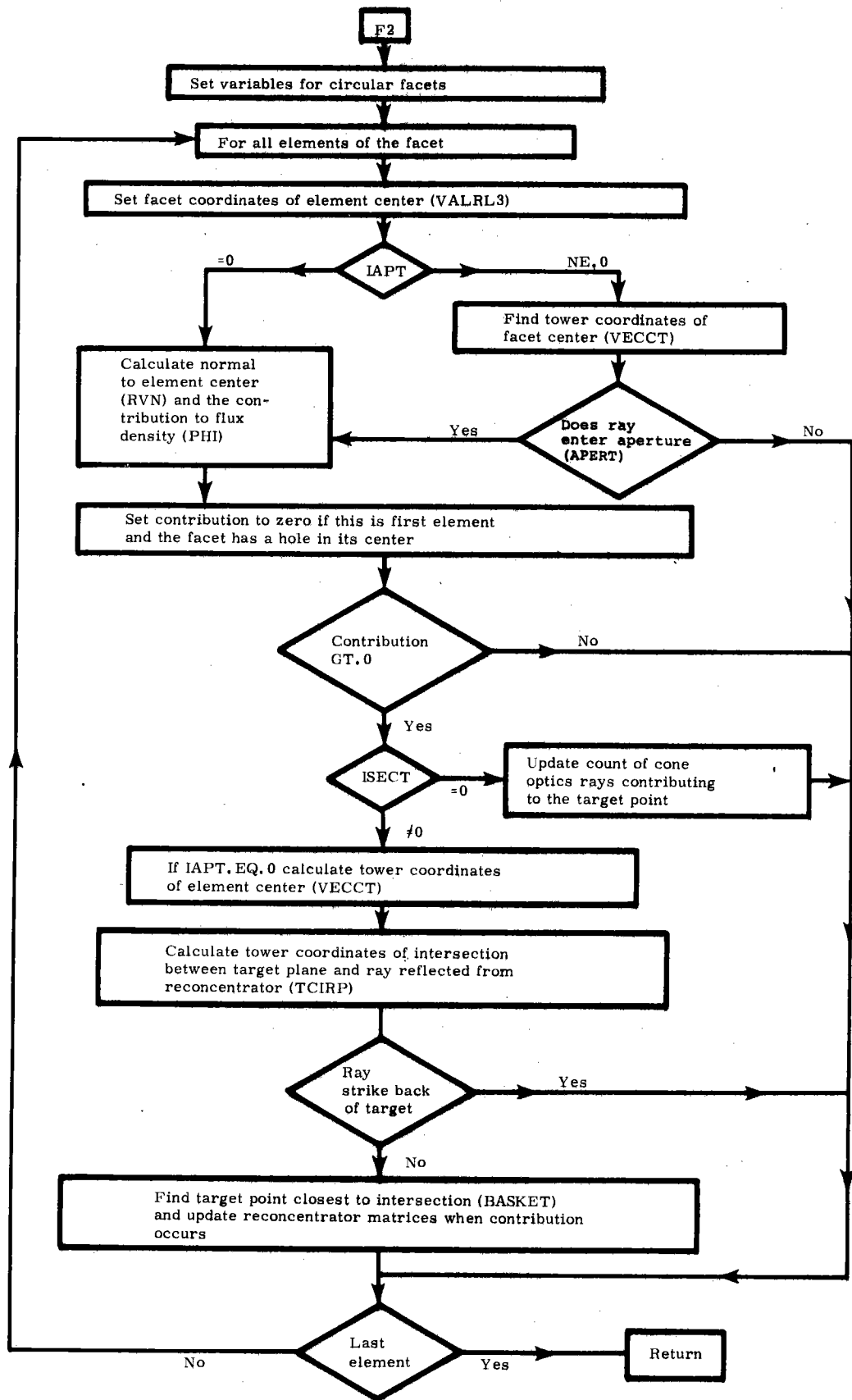
Part A

Figure A-4. Flow Diagram for FACET Function



Part B

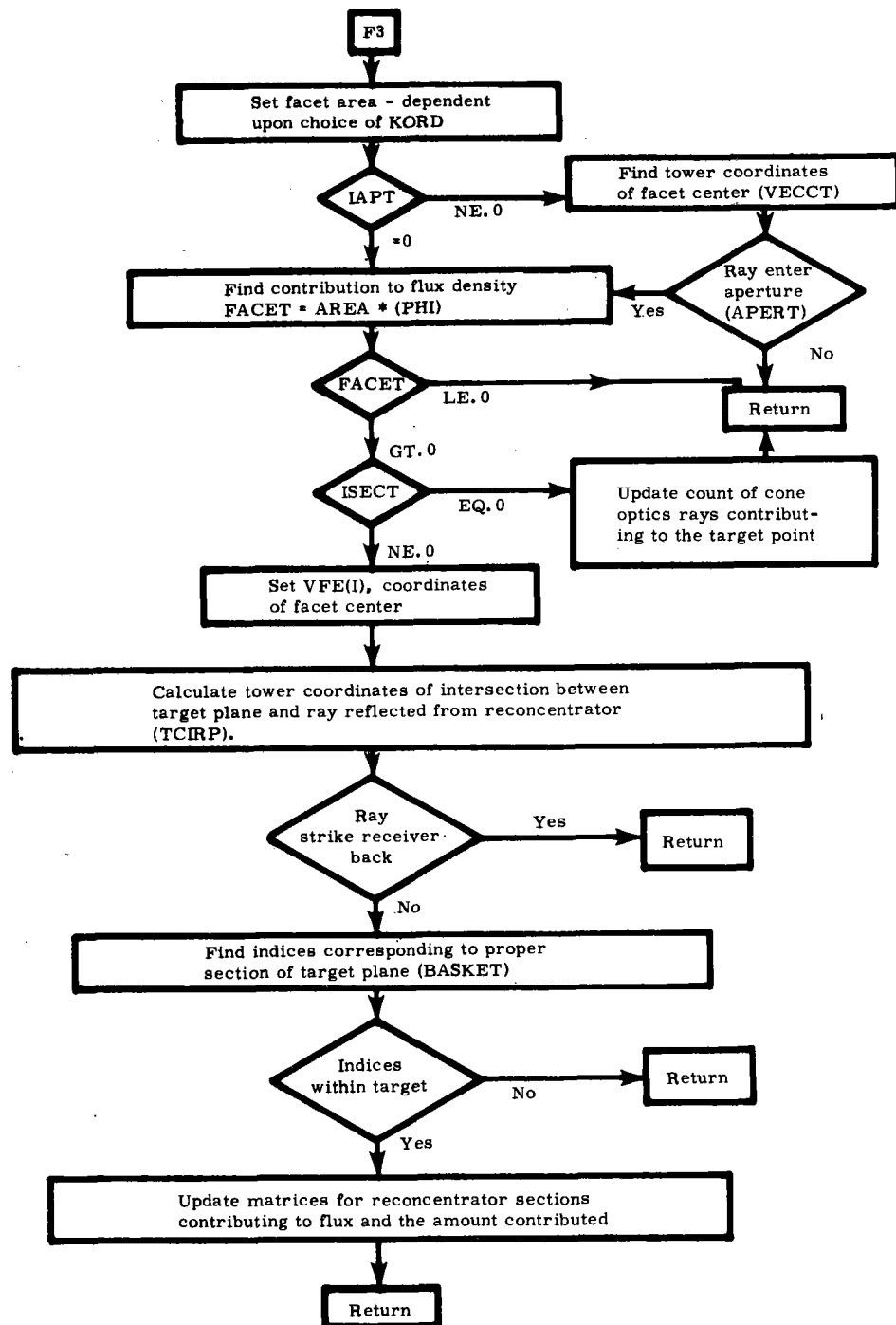
Figure A-4 (cont)



Part C

Part C

Figure A-4 (cont)



Part D

Figure A-4 (concluded)

FACETA(RB,VM), a reduced version of FACET, is called only from function FN. In turn, FN is used only in CPQR with Subroutine MINA. The function FACETA is only used when IOPT=3 or 4, indicating the facet shape is determined by stress analysis. When FACETA is in use, the Routine CPQR calls MINA to determine the pulldown distance at the back of the facet center that maximizes the flux density at the target point used for prealignment.

FF(X) evaluates the sunshape at $\rho=x$ in Program D for printout when ICON=1. The function is used by the function FZ to normalize the input sunshape, by the function FR as an aid to finding the rms width of the input sunshape, and by CONV for storing the sunshape distribution before convolution.

FFONE(R), which is identical to FF(X), evaluates the sunshape for numerical convolution with error-cone data. FFONE is called by NUCONV in the overlay controlled by Program C. (The FF is in the overlay controlled by Program D.)

FI(X) calculates the effective sunshape for given $X = \rho = \tan \alpha$ when ICON=1. Linear (INTERP=1) or cubic-spline (INTERP=2) interpolation is used between values of ρ tabulated after the numerical convolution. This function is called by CONE, CONEA, D, and by FIN.

FIN(X) evaluates X times FI(X). This function is called by Program D to normalize the effective sunshape by means of NORM.

FMAX(A,N) finds the maximum value of the first N elements of the one-dimensional matrix A. The function is called by Program C to find the maximum in the flux-density matrix for an individual heliostat.

FN(X) calculates the negative of FACET(RB,VM). The FN function is used in CPQR with Subroutine MINA to maximize the flux density at the focus point by varying the facet pulldown distance.

FOURT, an SNL mathematical program library subroutine, performs a fast-Fourier transform of an array of complex data. The subroutine is called by CONV and NUCONV for numerical convolution of error cones and sunshapes to obtain effective sunshapes. The library is discussed in Reference 3.

FPADJ(NHELI,HE,HN,HZ,HEFOC,HNFOC,HZFOC) calculates the aim point used for prealignment (canting) of heliostat number NHELI, with base coordinates HE,HN,HZ. The subroutine is called by Program A when IHELD=2. In its present form the desired coordinates HEFOC,HNFOC,HZFOC are obtained from Subroutine APADJ.

FR(X) evaluates $X^3*FF(X)$ where $X = \rho = \tan \alpha$. This function is used in Program D as a numerical-integration aid to find the mean-square width of the sunshape.

FRES(X), a function of $X = \rho = \tan \alpha$, normalizes (with the aid of NORMC) the effective sunshape evaluated by NUCONV when a one-dimensional effective sunshape is desired. FRES is called by function PHI.

FU(U),FV(V) ensure proper normalization of the effective sunshape when the two-dimensional effective sunshape is evaluated by fast-Fourier transforms (NUCONV). In function PHI the numerical integration routine QNC7 integrates FV(V) between the upper and lower V limits for nonzero values of the shape. In turn, the FV(V) function uses GAUSS to integrate FU(U) over the U variable at given value of V. The two-dimensional integration of the sunshape over the U-V (reflected-ray reference) plane is used to renormalize the two-dimensional matrix of effective sunshape probability-density functions (RESL(I,J)). Function FU is called only by FV. Function FV is called only by PHI.

FVOT(VIN,VN,VOT) uses the incident unit vector with components VIN(I=1,3) and the surface normal vector VN(I=1,3) to calculate the unit normal in the direction of the specularly reflected ray.

$$\underline{V}_{OT} = \underline{V}_{IN} - 2(\underline{V}_{IN} \cdot \underline{V}_N)\underline{V}_N$$

The function FVOT is called by CPQR, PHID, and by Program C.

FZ(X) calculates the $X*FF(X)$ where $X = \rho = \tan \alpha$. This function is used in Program D to normalize the sunshape by means of NORM.

GAUSS uses an adaptive 8-point Legendre-Gauss algorithm to numerically integrate real functions of one variable. The subroutine is part of the Sandia mathematical program library discussed in Reference 3. GAUSS is called only by FV and is used to integrate FU(U).

GETNSF(NF,THE,NSF) determines the unit vector normal to a given facet, including the effect of gravity (or wind) loading. The facet number (NF) and the heliostat elevation angle (THE in radians) are input parameters. The real, three-dimensional unit vector (NSF= \underline{N}_f) normal to the facet is returned as output. The subroutine is called by GLOAD. Because it is not discussed elsewhere and may require alteration for additional types of loading, more detailed discussion is included.

With given elevation angle, the subroutine first searches Tape 1 for loading data appropriate for the given facet (NF) that applies for elevation angles just larger (EL2) and just smaller (EL1) than THE. The loading data are stored in order of increasing elevation angles at 15° intervals from 0° to 105°. The appropriate facet normals are labeled VS1(I) and VS2(I), I=1,3. Subroutine GETNSF then interpolates between VS1 and VS2 to obtain the facet normal \hat{N}_f corresponding to elevation angle THE. A description of the interpolation follows.

The axis of rotation is obtained by the normalized cross product

$$\hat{C} = \underline{VS1} \times \underline{VS2} / |\underline{VS1} \times \underline{VS2}| \quad .$$

The angle of rotation between data points is

$$\delta_1 = \sin^{-1} |\underline{VS1} \times \underline{VS2}| \quad .$$

The angle of rotation between VS1 and the proper normal at elevation angle THE is

$$\delta = \delta_1 \frac{THE - EL1}{EL2 - EL1} \quad .$$

The rotation axis \hat{C} has direction cosines (C_1, C_2, C_3) . With the δ evaluated earlier, the \hat{N}_f is found by rotation of VS1 about \hat{C} through angle δ . This rotation is performed by Subroutine ROTAT.

To understand and use this method of accounting for loading effects, a user must know how Tape 1 is generated and how to obtain the Tape-1 file for a particular computer run. The data contained in Tape 1 are illustrated in Table A-1. The McDonnell-Douglas heliostat design (MDAC) has two columns of facets arranged in six rows. The table gives facet normals N_f for Facets 1 through 12. The facets are numbered from left to right as viewed facing the reflective surfaces, starting with the top row and continuing to the bottom. The corner facets are then 1, 2 12, 11 in clockwise order. The coordinate system is (x, y, z) for (east, north, vertical). The data in Table A-1 are generated by the NASTRAN computer code. They are stored on Tape 1 by using unformatted-write statements and the CDC7600 computer at SNLA. Parameter order on Tape 1 is facet number, elevation angle (rad), identification note, and the three components of the facet normal, with facet and angle order as in Table A-1. An example of Tape 1 is file MDAC-TAPE1-NASTRAN-SEPT79, which at this writing is on the CDC7600 permanent file system at SNL. No file card is necessary.

The Martin-Marietta heliostat also has two columns of facets arranged in six rows. The numbering scheme is as described above. The file for this data is MMC-TAPE1-NASTRAN-SEPT79 on the CDC7600 permanent file system at SNLA. This MMC heliostat has 12 facets. Note that in Table A-1 the NASTRAN results are presented with 45° elevation angle as a reference; i.e., gravity-loading effects have been compensated for at 45°. The treatment of canting in HELIOS allows this compensation to occur for whatever elevation angle exists at prealignment time.

The example in Table A-1 records elevation angles in degrees. Before Tape 1 was actually generated, the degrees were converted to radians for consistency with the use of elevation angle, THE, in HELIOS.

TABLE A-1

Tape 1 Data From NASTRAN

McDonnell-Douglas Heliostats

Facet	Elevation Angle (Degrees)		Normal to Facet		
			x	y	z
1	0.0000	MDAC NORM	.486705E-03	-.100000E+01	-.506000E-03
2	0.0000	MDAC NORM	-.486207E-03	-.100000E+01	-.505849E-03
3	0.0000	MDAC NORM	.447154E-03	-.100000E+01	-.292132E-03
4	0.0000	MDAC NORM	-.447256E-03	-.100000E+01	-.292168E-03
5	0.0000	MDAC NORM	.420892E-03	-.100000E+01	-.224500E-03
6	0.0000	MDAC NORM	-.420860E-03	-.100000E+01	-.224526E-03
7	0.0000	MDAC NORM	.402390E-03	-.100000E+01	.903416E-04
8	0.0000	MDAC NORM	-.402393E-03	-.100000E+01	.902985E-04
9	0.0000	MDAC NORM	.399356E-03	-.100000E+01	.164787E-03
10	0.0000	MDAC NORM	-.399250E-03	-.100000E+01	.164751E-03
11	0.0000	MDAC NORM	.410135E-03	-.100000E+01	.357839E-03
12	0.0000	MDAC NORM	-.410639E-03	-.100000E+01	.358055E-03
1	15.0000	MDAC NORM	.318061E-03	-.966016E+00	.258483E+00
2	15.0000	MDAC NORM	-.317746E-03	-.966016E+00	.258483E+00
3	15.0000	MDAC NORM	.289470E-03	-.965980E+00	.258617E+00
4	15.0000	MDAC NORM	-.289535E-03	-.965980E+00	.258617E+00
5	15.0000	MDAC NORM	.269150E-03	-.965969E+00	.258657E+00
6	15.0000	MDAC NORM	-.269126E-03	-.965969E+00	.258657E+00
7	15.0000	MDAC NORM	.252804E-03	-.965918E+00	.258850E+00
8	15.0000	MDAC NORM	-.252803E-03	-.965918E+00	.258850E+00
9	15.0000	MDAC NORM	.247206E-03	-.965905E+00	.258896E+00
10	15.0000	MDAC NORM	-.247139E-03	-.965905E+00	.258896E+00
11	15.0000	MDAC NORM	.250523E-03	-.965874E+00	.259012E+00
12	15.0000	MDAC NORM	-.250843E-03	-.965874E+00	.259012E+00
1	30.0000	MDAC NORM	.152043E-03	-.866103E+00	.499865E+00
2	30.0000	MDAC NORM	-.151898E-03	-.866103E+00	.499865E+00
3	30.0000	MDAC NORM	.136943E-03	-.866071E+00	.499921E+00
4	30.0000	MDAC NORM	-.136973E-03	-.866071E+00	.499921E+00
5	30.0000	MDAC NORM	.125581E-03	-.866061E+00	.499938E+00
6	30.0000	MDAC NORM	-.125568E-03	-.866061E+00	.499938E+00
7	30.0000	MDAC NORM	.115546E-03	-.866015E+00	.500018E+00
8	30.0000	MDAC NORM	-.115544E-03	-.866015E+00	.500018E+00
9	30.0000	MDAC NORM	.110984E-03	-.866004E+00	.500037E+00
10	30.0000	MDAC NORM	-.110952E-03	-.866004E+00	.500037E+00
11	30.0000	MDAC NORM	.110624E-03	-.865977E+00	.500084E+00
12	30.0000	MDAC NORM	-.110772E-03	-.865977E+00	.500084E+00
1	45.0000	MDAC NORM	0.	-.707107E+00	.707107E+00
2	45.0000	MDAC NORM	0.	-.707107E+00	.707107E+00
3	45.0000	MDAC NORM	0.	-.707107E+00	.707107E+00
4	45.0000	MDAC NORM	0.	-.707107E+00	.707107E+00
5	45.0000	MDAC NORM	0.	-.707107E+00	.707107E+00
6	45.0000	MDAC NORM	0.	-.707107E+00	.707107E+00
7	45.0000	MDAC NORM	0.	-.707107E+00	.707107E+00
8	45.0000	MDAC NORM	0.	-.707107E+00	.707107E+00
9	45.0000	MDAC NORM	0.	-.707107E+00	.707107E+00
10	45.0000	MDAC NORM	0.	-.707107E+00	.707107E+00
11	45.0000	MDAC NORM	0.	-.707107E+00	.707107E+00
12	45.0000	MDAC NORM	0.	-.707107E+00	.707107E+00
1	60.0000	MDAC NORM	-.127726E-03	-.499879E+00	.866095E+00
2	60.0000	MDAC NORM	.127616E-03	-.499879E+00	.866095E+00
3	60.0000	MDAC NORM	-.112046E-03	-.499925E+00	.866069E+00
4	60.0000	MDAC NORM	.112068E-03	-.499925E+00	.866069E+00
5	60.0000	MDAC NORM	-.990518E-04	-.499937E+00	.866062E+00
6	60.0000	MDAC NORM	.990378E-04	-.499937E+00	.866062E+00
7	60.0000	MDAC NORM	-.859775E-04	-.499998E+00	.866026E+00
8	60.0000	MDAC NORM	.859715E-04	-.499998E+00	.866026E+00
9	60.0000	MDAC NORM	-.781980E-04	-.500014E+00	.866017E+00
10	60.0000	MDAC NORM	.781733E-04	-.500014E+00	.866017E+00
11	60.0000	MDAC NORM	-.738265E-04	-.500047E+00	.865998E+00
12	60.0000	MDAC NORM	.739409E-04	-.500047E+00	.865998E+00
1	75.0000	MDAC NORM	-.222433E-03	-.258570E+00	.965992E+00
2	75.0000	MDAC NORM	.222254E-03	-.258570E+00	.965992E+00

TABLE A-1--Continued

Facet	Elevation Angle (Degrees)		Normal to Facet		
			x	y	z
3	75.0000	MDAC NORM	-.191559E-03	-.258657E+00	.965969E+00
4	75.0000	MDAC NORM	.191594E-03	-.258657E+00	.965969E+00
5	75.0000	MDAC NORM	-.164825E-03	-.258677E+00	.965964E+00
6	75.0000	MDAC NORM	.164797E-03	-.258677E+00	.965964E+00
7	75.0000	MDAC NORM	-.136528E-03	-.258788E+00	.965934E+00
8	75.0000	MDAC NORM	.136512E-03	-.258788E+00	.965934E+00
9	75.0000	MDAC NORM	-.118282E-03	-.258818E+00	.965926E+00
11	75.0000	MDAC NORM	.118241E-03	-.258818E+00	.965926E+00
11	75.0000	MDAC NORM	-.105824E-03	-.258875E+00	.965911E+00
12	75.0000	MDAC NORM	.106012E-03	-.258875E+00	.965911E+00
1	90.0000	MDAC NORM	-.277662E-03	.343046E-03	.100000E+01
2	90.0000	MDAC NORM	.277461E-03	.343049E-03	.100000E+01
3	90.0000	MDAC NORM	-.233118E-03	.233896E-03	.100000E+01
4	90.0000	MDAC NORM	.233157E-03	.233912E-03	.100000E+01
5	90.0000	MDAC NORM	-.192835E-03	.212704E-03	.100000E+01
6	90.0000	MDAC NORM	.192794E-03	.212697E-03	.100000E+01
7	90.0000	MDAC NORM	-.148202E-03	.822767E-04	.100000E+01
8	90.0000	MDAC NORM	.148176E-03	.823119E-04	.100000E+01
9	90.0000	MDAC NORM	-.117516E-03	.446382E-04	.100000E+01
11	90.0000	MDAC NORM	.117469E-03	.446520E-04	.100000E+01
11	90.0000	MDAC NORM	-.938104E-04	-.146968E-04	.100000E+01
12	90.0000	MDAC NORM	.940242E-04	-.148518E-04	.100000E+01
1	105.0000	MDAC NORM	-.289650E-03	.259182E+00	.965828E+00
2	105.0000	MDAC NORM	.289476E-03	.259182E+00	.965828E+00
3	105.0000	MDAC NORM	-.233891E-03	.259077E+00	.965856E+00
4	105.0000	MDAC NORM	.233923E-03	.259077E+00	.965856E+00
5	105.0000	MDAC NORM	-.181174E-03	.259063E+00	.965860E+00
6	105.0000	MDAC NORM	.181120E-03	.259063E+00	.965860E+00
7	105.0000	MDAC NORM	-.120208E-03	.258952E+00	.965890E+00
8	105.0000	MDAC NORM	.120167E-03	.258952E+00	.965890E+00
9	105.0000	MDAC NORM	-.759559E-04	.258916E+00	.965900E+00
11	105.0000	MDAC NORM	.759120E-04	.258916E+00	.965900E+00
11	105.0000	MDAC NORM	-.386057E-04	.258877E+00	.965910E+00
12	105.0000	MDAC NORM	.387977E-04	.258877E+00	.965910E+00

Martin-Marietta Heliostats

Facet	Elevation Angle (Degrees)		Normal to Facet		
			x	y	z
1	0.0000	MNC NORM	.315001E-03	-.100000E+01	-.121835E-03
2	0.0000	MNC NORM	-.320677E-03	-.100000E+01	-.129673E-03
3	0.0000	MNC NORM	.373977E-03	-.100000E+01	-.109296E-03
4	0.0000	MNC NORM	-.374317E-03	-.100000E+01	-.117455E-03
5	0.0000	MNC NORM	.465702E-03	-.100000E+01	.116817E-04
6	0.0000	MNC NORM	-.412989E-03	-.100000E+01	.303524E-05
7	0.0000	MNC NORM	.564566E-03	-.100000E+01	.233618E-03
8	0.0000	MNC NORM	-.414669E-03	-.100000E+01	.224980E-03
9	0.0000	MNC NORM	.668542E-03	-.100000E+01	.347856E-03
10	0.0000	MNC NORM	-.468277E-03	-.100000E+01	.339619E-03
11	0.0000	MNC NORM	.734255E-03	-.100000E+01	.342498E-03
12	0.0000	MNC NORM	-.536333E-03	-.100000E+01	.334294E-03
1	15.0000	MNC NORM	.202886E-03	-.965947E+00	.258740E+00
2	15.0000	MNC NORM	-.211814E-03	-.965948E+00	.258736E+00
3	15.0000	MNC NORM	.237171E-03	-.965945E+00	.258749E+00
4	15.0000	MNC NORM	-.241818E-03	-.965946E+00	.258745E+00
5	15.0000	MNC NORM	.296643E-03	-.965922E+00	.258832E+00
6	15.0000	MNC NORM	-.263833E-03	-.965924E+00	.258827E+00
7	15.0000	MNC NORM	.351659E-03	-.965887E+00	.258963E+00
8	15.0000	MNC NORM	-.259283E-03	-.965889E+00	.258959E+00
9	15.0000	MNC NORM	.416544E-03	-.965870E+00	.259027E+00
10	15.0000	MNC NORM	-.294843E-03	-.965871E+00	.259023E+00
11	15.0000	MNC NORM	.454742E-03	-.965872E+00	.259023E+00
12	15.0000	MNC NORM	-.335160E-03	-.965873E+00	.259019E+00

TABLE A-1--Continued

Facet	Elevation Angle (Degrees)		Normal to Facet		
			x	y	z
1	30.0000 MMC	NORM	.954476E-04	-.866048E+00	.499961E+00
2	30.0000 MMC	NORM	-.102439E-03	-.866049E+00	.499959E+00
3	30.0000 MMC	NORM	.109617E-03	-.866045E+00	.499966E+00
4	30.0000 MMC	NORM	-.114148E-03	-.866046E+00	.499964E+00
5	30.0000 MMC	NORM	.137804E-03	-.866023E+00	.500004E+00
6	30.0000 MMC	NORM	-.122973E-03	-.866024E+00	.500002E+00
7	30.0000 MMC	NORM	.159100E-03	-.865993E+00	.500056E+00
8	30.0000 MMC	NORM	-.117850E-03	-.865994E+00	.500055E+00
9	30.0000 MMC	NORM	.188522E-03	-.865979E+00	.500080E+00
10	30.0000 MMC	NORM	-.135126E-03	-.865980E+00	.500078E+00
11	30.0000 MMC	NORM	.204307E-03	-.865981E+00	.500077E+00
12	30.0000 MMC	NORM	-.152231E-03	-.865982E+00	.500076E+00
1	45.0000 MMC	NORM	0.	-.707107E+00	.707107E+00
2	45.0000 MMC	NORM	0.	-.707107E+00	.707107E+00
3	45.0000 MMC	NORM	0.	-.707107E+00	.707107E+00
4	45.0000 MMC	NORM	0.	-.707107E+00	.707107E+00
5	45.0000 MMC	NORM	0.	-.707107E+00	.707107E+00
6	45.0000 MMC	NORM	0.	-.707107E+00	.707107E+00
7	45.0000 MMC	NORM	0.	-.707107E+00	.707107E+00
8	45.0000 MMC	NORM	0.	-.707107E+00	.707107E+00
9	45.0000 MMC	NORM	0.	-.707107E+00	.707107E+00
10	45.0000 MMC	NORM	0.	-.707107E+00	.707107E+00
11	45.0000 MMC	NORM	0.	-.707107E+00	.707107E+00
12	45.0000 MMC	NORM	0.	-.707107E+00	.707107E+00
1	60.0000 MMC	NORM	-.769509E-04	-.499959E+00	.866049E+00
2	60.0000 MMC	NORM	.885210E-04	-.499959E+00	.866049E+00
3	60.0000 MMC	NORM	-.842085E-04	-.499965E+00	.866046E+00
4	60.0000 MMC	NORM	.928453E-04	-.499964E+00	.866046E+00
5	60.0000 MMC	NORM	-.107376E-03	-.500003E+00	.866024E+00
6	60.0000 MMC	NORM	.967048E-04	-.500002E+00	.866024E+00
7	60.0000 MMC	NORM	-.114798E-03	-.500038E+00	.866003E+00
8	60.0000 MMC	NORM	.862339E-04	-.500039E+00	.866003E+00
9	60.0000 MMC	NORM	-.136172E-03	-.500050E+00	.865996E+00
10	60.0000 MMC	NORM	.101325E-03	-.500050E+00	.865996E+00
11	60.0000 MMC	NORM	-.144253E-03	-.500047E+00	.865998E+00
12	60.0000 MMC	NORM	.111156E-03	-.500047E+00	.865998E+00
1	75.0000 MMC	NORM	-.130163E-03	-.258718E+00	.965953E+00
2	75.0000 MMC	NORM	.157094E-03	-.258719E+00	.965953E+00
3	75.0000 MMC	NORM	-.137272E-03	-.258731E+00	.965949E+00
4	75.0000 MMC	NORM	.158064E-03	-.258732E+00	.965949E+00
5	75.0000 MMC	NORM	-.177010E-03	-.258813E+00	.965927E+00
6	75.0000 MMC	NORM	.160554E-03	-.258813E+00	.965927E+00
7	75.0000 MMC	NORM	-.177472E-03	-.258871E+00	.965912E+00
8	75.0000 MMC	NORM	.134977E-03	-.258871E+00	.965912E+00
9	75.0000 MMC	NORM	-.210717E-03	-.258884E+00	.965908E+00
10	75.0000 MMC	NORM	.161945E-03	-.258885E+00	.965908E+00
11	75.0000 MMC	NORM	-.218625E-03	-.258875E+00	.965910E+00
12	75.0000 MMC	NORM	.173666E-03	-.258876E+00	.965910E+00
1	90.0000 MMC	NORM	-.156007E-03	.160740E-03	.100000E+01
2	90.0000 MMC	NORM	.201043E-03	.157015E-03	.100000E+01
3	90.0000 MMC	NORM	-.155570E-03	.139077E-03	.100000E+01
4	90.0000 MMC	NORM	.191206E-03	.135963E-03	.100000E+01
5	90.0000 MMC	NORM	-.204150E-03	.193566E-04	.100000E+01
6	90.0000 MMC	NORM	.187190E-03	.172940E-04	.100000E+01
7	90.0000 MMC	NORM	-.183745E-03	-.359347E-04	.100000E+01
8	90.0000 MMC	NORM	.142903E-03	-.380576E-04	.100000E+01
9	90.0000 MMC	NORM	-.218548E-03	-.343962E-04	.100000E+01
10	90.0000 MMC	NORM	.17725E-03	-.376025E-04	.100000E+01
11	90.0000 MMC	NORM	-.218039E-03	-.203685E-04	.100000E+01
12	90.0000 MMC	NORM	.183262E-03	-.238430E-04	.100000E+01
1	105.0000 MMC	NORM	-.152721E-03	.259018E+00	.965872E+00
2	105.0000 MMC	NORM	.21372E-03	.259011E+00	.965874E+00
3	105.0000 MMC	NORM	-.137855E-03	.258991E+00	.965880E+00
4	105.0000 MMC	NORM	.190013E-03	.258984E+00	.965881E+00
5	105.0000 MMC	NORM	-.186947E-03	.258849E+00	.965918E+00
6	105.0000 MMC	NORM	.174800E-03	.258844E+00	.965919E+00
7	105.0000 MMC	NORM	-.133190E-03	.258823E+00	.965925E+00

TABLE A-1--Continued

Facet	Elevation Angle (Degrees)		Normal to Facet		
			x	y	z
8	105.0000MMC	NORM	.109473E-03	.258818E+00	.965926E+00
9	105.0000MMC	NORM	-.159130E-03	.258851E+00	.965917E+00
10	105.0000MMC	NORM	.147589E-03	.258845E+00	.965919E+00
11	105.0000MMC	NORM	-.142535E-03	.258870E+00	.965912E+00
12	105.0000MMC	NORM	.139292E-03	.258863E+00	.965914E+00

As an example, let us examine the first facet when the elevation angle is 15°. The heliostat is facing south, with heliostat unit normal (0., -0.965926, +0.258819). Facet 1 has unit normal (0.00318, -0.966016, 0.258483). The facet normal has sagged slightly downward and inward to the east. The heliostat design would suggest that Facet 2 should sag a corresponding amount downward and to the west; this is true up to the seventh-decimal place. The small lack of symmetry indicated is thought to result from computer roundoff error in NASTRAN. The normals in Table A-1 lead us to expect that loading effects will spread intensity patterns horizontally and either lower or raise the positions of peak flux density in the power distribution produced by each heliostat (depending upon heliostat elevation angles at calculation time and at canting time).

Some temporary convenience might be gained by storing the Tape 1 data in HELIOS-Code statements. However, it was judged more convenient to alter heliostat designs by altering data on Tape 1 rather than the code. Card input would require simultaneous storage space for all the data. Future applications may specify gravity-loading distortions from NASTRAN for many points on each facet (rather than just the center). So the required storage space could become large. The method illustrated here requires little additional storage in HELIOS, even for such more-detailed applications.

GG(X) evaluates the error-cone probability-density distribution. The function is called by Program D for printing the error cone, by CONV to fill in the error-cone matrix before numerical convolution to obtain the effective sun-shape, by GN as an aid in normalization of the distribution, and by GR as an aid to finding the mean-square width of the error cone.

GLOAD(VN,ELEVA,THE,NF,CELEVA,SELEVA,CPHIH,SPHIH,CTHE,STHE) controls the treatment of gravity- or wind-loading of the heliostat. Here the facets are treated as rigid bodies that are rotated slightly by the loading effects. The method is not optimized for speed. If extensive application to large heliostat fields is expected to be expensive, considerable reduction in time is possible.

Upon input to Subroutine GLOAD VN(I,NF), I=1,3 gives the components of the unit normal (in the tower coordinate system) to the individual facet with index NF.

$$\hat{n}_i = VN(I, NF), I=1,3 \quad .$$

The heliostat elevation and azimuth angles are ξ_e (THE with cosine and sine CTHE and STHE) and ϕ_e (with cosine and sine CPHIH and SPHIH). The elevation angle at prealignment is ξ_p (ELEVA). Since ϕ_e is measured from the east (positive to the north) and ξ_e is measured upward from the horizontal, the unit normal to the heliostat is given by

$$n_x = \cos \xi_e \cos \phi_e \quad ,$$

$$n_y = \cos \xi_e \sin \phi_e \quad ,$$

$$n_z = \sin \xi_e \quad .$$

GLOAD must furnish a new value of the facet normal, designated by \hat{n}_f , that includes the effect of gravity loading. The heliostat coordinate system is assumed to remain unchanged. Loading may displace each facet center. However, such displacements are ignored, allowing the transformation to be described by a rotation matrix A:

$$\hat{n}_f = A \hat{n}_i \quad .$$

The rotation matrix must be determined from loading data and from the particular heliostat elevation and azimuthal angles.

We assume that loading results are furnished in a coordinate system with x, y, z representing the east, north, and vertical directions, and where the horizontal axis of the north-field heliostat is in the east-west direction (azimuthal angle for heliostat normal = $-\pi/2$). The individual facets have unit normals given by \hat{N}_i and \hat{N}_f before and after loading effects are included.

$$\hat{N}_f = A \hat{N}_i \quad .$$

A unit vector along the axis of rotation is given by the normalized cross product

$$\hat{C}_N = \hat{N}_i \times \hat{N}_f / |\hat{N}_i \times \hat{N}_f| \quad ,$$

while the angle of rotation is

$$\delta_N = \sin^{-1} |\hat{N}_i \times \hat{N}_f| \quad .$$

The subscript N indicates loading effect based upon loading (NASTRAN) calculations. We cannot apply the same rotation to the individual facets to transform from \hat{n}_i to \hat{n}_f .

The azimuthal angle used by NASTRAN is not necessarily the same as that for a particular heliostat in a HELIOS calculation. The rotation axis varies with the location of the heliostat. A rotation through angle ϕ_r about a vertical axis converts to the appropriate axis \hat{C}_1 .

$$\hat{C}_1 = B \hat{C}_N$$

where

$$B = \begin{pmatrix} \cos \phi_r & -\sin \phi_r & 0 \\ \sin \phi_r & \cos \phi_r & 0 \\ 0 & 0 & 1 \end{pmatrix} .$$

The $\phi_r = \phi_e - \phi_N$ where ϕ_e is the heliostat azimuthal angle in HELIOS and ϕ_N is the heliostat azimuthal angle used in the loading calculations. Earlier, ϕ_N was assumed to be $-\pi/2$. The \hat{n}_i -to- \hat{n}_f rotation is now obtained from

$$\hat{n}_f = \hat{n}_i + (\hat{C}_1 \times \hat{n}_i) \delta_N .$$

This expression assumes δ_N is small and is described by G. A. Korn and T. M. Korn.⁴

If the heliostat is properly canted with elevation angle ELEVA (cosine and sine CELEVA and SELEVA) at canting time, then the loading has been included in the canting of each facet. Hence, the above equation must be applied again to include rotation during canting. In GLOAD this is done by calculating \hat{C}_N' , \hat{C}_1' , and δ_N' appropriate for elevation angle ELEVA. Equation 4 is then applied a second time with δ_N' replaced by its negative. This method allows for the possibility that the rotation axis (\hat{C}_1) can vary with the elevation angle.

As a further example of GLOAD's effect, Table A-2 lists the McDonnell-Douglas facet normals before and after calls to GLOAD for the special case of elevation angle 50° and heliostat azimuthal angles 0° and $-\pi/2$. The elevation angle used to set the canting is taken as $ELEVA=5^\circ$. Here the original normal is taken as the normal to the heliostat itself. GLOAD has rotated the normals horizontally outward and upward from the original facet normals.

GLOAD treats the facets as rigid bodies rotated slightly by loading effects. An alternative is to allow the facet shape to become distorted. This approach would require much more elaborate data on Tape 1 and corresponding complexity in the interpolation routine.

TABLE A-2

Facet Normals Before and After Calls to GLOAD for
One McDonnell-Douglas Heliostat Design

<u>NF</u>	<u>VN(1)</u>	<u>VN(2)</u>	<u>VN(3)</u>	<u> VN </u>	<u>N</u>	<u>N'</u>
Heliostat azimuthal angle is 0.000000.						
Heliostat elevation angle is 0.872665 rad.						
Each facet has original VN = 0.642788, 0.000000, 0.766044.						
1	0.642405	-0.000350	0.766366	1.000000	0.000063	-0.000627
2	0.642405	0.000349	0.766366	1.000000	0.000063	-0.000627
3	0.642563	-0.000319	0.766233	1.000000	0.000048	-0.000477
4	0.642563	0.000319	0.766233	1.000000	0.000048	-0.000478
5	0.642612	-0.000297	0.766192	1.000000	0.000041	-0.000426
6	0.642612	0.000297	0.766192	1.000000	0.000041	-0.000426
7	0.642841	-0.000280	0.765999	1.000000	0.000029	-0.000362
8	0.642841	0.000280	0.765999	1.000000	0.000029	-0.000362
9	0.642396	-0.000275	0.765953	1.000000	0.000027	-0.000377
10	0.642896	0.000275	0.765953	1.000000	0.000027	-0.000377
11	0.643035	-0.000279	0.765837	1.000000	0.000031	-0.000472
12	0.643035	0.000279	0.765837	1.000000	0.000031	-0.000472

Heliostat azimuthal angle is -1.570796 rad.
Heliostat elevation angle is 0.872665 rad.
Each facet has original VN = -0.000000, -0.642788, 0.766044.

1	-0.000350	-0.642405	0.766366	1.000000	0.000063	-0.000627
2	-0.000349	-0.642405	0.766366	1.000000	0.000063	-0.000627
3	-0.000319	-0.642563	0.766233	1.000000	0.000048	-0.000477
4	0.000319	-0.642563	0.766233	1.000000	0.000048	-0.000478
5	-0.000297	-0.642612	0.766192	1.000000	0.000041	-0.000426
6	0.000297	-0.642612	0.766192	1.000000	0.000041	-0.000426
7	-0.000280	-0.642841	0.765999	1.000000	0.000029	-0.000362
8	0.000280	-0.642841	0.765999	1.000000	0.000029	-0.000362
9	-0.000275	-0.642896	0.765953	1.000000	0.000027	-0.000377
10	0.000275	-0.642896	0.765953	1.000000	0.000027	-0.000377
11	-0.000279	-0.643035	0.765837	1.000000	0.000031	-0.000472
12	0.000279	-0.643035	0.765837	1.000000	0.000031	-0.000472

GN(X) evaluates $X*GG(X)$. The function is called by Program D to normalize the error cone by means of NORM.

GR(X) evaluates $X^3*GG(X)$. The function is called by Program D to find the mean-square width of the error cone by means of the numerical integration routine QNC7. GR is used only when ICON=1.

INDATA(NCALL) reads all the input data required for a HELIOS calculation. Data statements in this subroutine give the tower coordinates (HDM(I,J),J=1,3) for heliostat-base position numbers I=1,504 at the Central Receiver Test Facility (CRTF). The routine is called by Program A. Part I of the user's guide⁵ concentrates upon the many input parameters that may be defined by INDATA.

INTRP1(XVAL,YVAL,YPVAL,X,Y,N,ICONT) interpolates the table of values X(I), Y(I), I=1,N at the point X=XVAL. The resulting value is returned in YVAL. ICONT=0 gives linear interpolation. ICONT=1 uses piecewise cubic fits that are continuously differentiable, but does not return the value of the derivative (YPVAL) at XVAL. ICONT=2 is as for value 1 except for return of YVPAL. This

routine was written by R. E. Jones of Sandia's Computer Consulting and Training Division. This subroutine is called by PHI.

INTRVL(X,NX,XVAL,I,IERR), a binary search subroutine, provides the index I appropriate for the X(I) in the matrix X(J), J=1,NX that is just smaller than (or equal to) the input value X=XVAL. IERR is an error index. This subroutine is called by VAL2D. The values of X must be strictly increasing.

JITTER models the somewhat jerky motion of the heliostat azimuthal and elevation drive motors caused by the encoder least-count. After HELIOS calculates the proper heliostat angles, the jitter option adjusts each heliostat elevation and azimuthal angle so that it is in error by a random number uniformly distributed in the interval [0.,1.] times the encoder least-count. This option is expected to account for aiming error in a more realistic way when calculations are done for a large number of heliostats.

The treatment of uncertainties in HELIOS assumes that all variables contributing to the uncertainty in the normal to a facet at a particular point on the facet are randomly distributed. Several of the uncertainties are not random variables with zero bias, but suffer from biases that are not known at present.

Consider an aim point at the CRTF. The heliostat azimuth and elevation angles are measured by encoders with a least-count of 0.768 mrad. These angles are interrogated once per second. If the computer senses the angles are in error by more than 0.768 mrad, the motors are engaged to correct the heliostat orientation. The aiming thus has a jitter resulting from encoder least-count and from interrogation frequency. While the motors are stationary, the image formed by a particular heliostat drifts eastward (because of solar motion to the west) and upward and downward (dependent upon whether the sun is falling or rising). Thus the aim point has an average bias toward the east.

Heliostat 142 at the back of the north field at the CRTF has tower coordinates (-4.88, 194.77, 0.58 m). A target 44 m up on the tower is 200 m from that heliostat. A 0.768-mrad error in aim point would cause 0.308-m jitter in the center of the image. If this same error occurred in both azimuth and elevation angles, the translation would be larger. With a series of heliostats, we might expect to have each angle in error by a random amount varying from 0. to 0.768 mrad. This jitter should add a skewness to the image on the target as seen on several experimental measurements to date.

As a model of such aim-point difficulties, we

1. Calculate heliostat elevation and azimuthal angles.
2. Alter each angle between 0 and 0.768 mrad with the change determined by a random-number generator that would cause the image to move to the east and up or down (dependent upon time of day).

3. Continue the calculation.

The added Step 2 is furnished by Subroutine JITTER.

The heliostat elevation and azimuthal angles are calculated in Subroutine AZELB in the overlay controlled by Program B. AZELB originally calculated the heliostat elevation (ξ_h) and azimuthal (ϕ_h) angles.

$$\text{THE} = \xi_h \quad ,$$

$$\text{CTHE} = \cos \xi_h \quad ,$$

$$\text{STHE} = \sin \xi_h \quad ,$$

$$\text{CPHIH} = \cos \phi_h \quad ,$$

$$\text{SPHIH} = \sin \phi_h \quad .$$

As with all azimuthal angles in HELIOS, they are measured from the east, positive toward the north.

Let R_i be a random number chosen from a uniform distribution on $[0,1]$. The subscript becomes e(a) for elevation (azimuthal) angle. Let the encoder least-count be ℓ_e , ℓ_a for elevation and azimuthal angles. After the ξ_h and ϕ_h variables are calculated, the angles are altered by the prescription.

$$\xi'_h = \xi_h - \Delta\xi_h \quad ,$$

$$\phi'_h = \phi_h - \Delta\phi_h \quad ,$$

with $\Delta\xi_h = \pm R_e \ell_e$, $\Delta\phi_h = \pm R_a \ell_a$. The choice of sign is discussed later. HELIOS uses several other variables that are altered by the change. The normal to the heliostat must be recalculated.

$$\text{ETA1} = \text{CTHE} * \text{CPHIH} \quad ,$$

$$\text{ETA2} = \text{CTHE} * \text{SPHIH} \quad ,$$

$$\text{ETA3} = \text{STHE} \quad .$$

The coordinates of the heliostat center can be improved*

$$\text{X1} = \text{HE} + \text{HL1} * \text{ETA1} \quad ,$$

*Eq 3.2-1 in Reference 1.

$$Y1 = HN + HL1 * ETA2 ,$$

$$Z1 = HZ + HL2 + HL1 * ETA3 .$$

These are the only variables in HELIOS directly altered by the changes in heliostat orientation. (The aim-point variables such as ZETAT in Subroutine AZELB are used only to find the heliostat alignment.)

The choice of sign becomes involved if the prescription is to apply to heliostats to the south, north, east, and west of the tower with complete freedom in the choices of aim point and observation time. The purpose of the sign is to alter each angle backward along the path taken as the sun traverses the sky. Rather than add a series of tests to find the right sign, the sign is determined by finding the appropriate angles at a slightly earlier time.

Equation 3.2-7 in Reference 1 indicates

$$\tan \phi_h = \frac{\cos \xi_h \sin \phi_s + \cos \xi_t \sin \phi_t}{\cos \xi_s \cos \phi_s + \cos \xi_t \cos \phi_t} .$$

If the numerator and denominator are defined to be n and d, the elevation angle is given by

$$\tan \xi_h = \frac{\sin \xi_s + \sin \xi_t}{(n^2 + d^2)^{1/2}} .$$

Further restrictions are

$$-\pi/2 \leq \xi_h \leq \pi ,$$

$$-\pi < \phi_h \leq \pi .$$

Using these equations, we

- Step time backward by a small amount
- Calculate old solar angles ϕ_s old and ξ_s old
- Using old values of ϕ_t , ξ_t , find ξ_h old, ϕ_h old

then

$$\Delta \xi_h = R_e \ell_e \frac{\xi_h \text{ old} - \xi_h}{|\xi_h \text{ old} - \xi_h|} ,$$

$$\Delta\phi_h = R_a \ell_a \frac{\phi_{h \text{ old}} - \phi_h}{|\phi_{h \text{ old}} - \phi_h|} .$$

The solar angles are evaluated by Eqs 3.1-4 through 3.1-13 in Reference 1. As indicated earlier, the new angles are then

$$\xi'_h = \xi_h - \Delta\xi_h$$

$$\phi'_h = \phi_h - \Delta\phi_h .$$

MASON(QN,QO,AREA) calculates the area (AREA) of intersection for two (possibly) overlapping quadrilaterals. The x,y coordinates of the corners for the two quadrilaterals are QN(I,J) and QO(I,J). The I index varies from 1 to 4 for the four corners, while J varies from 1 to 2 identifying the x,y coordinates. This subroutine, written by D. S. Mason, is discussed in Reference 6. Application of MASON in HELIOS is discussed in Reference 1 in Sections 7.4.2 through 7.4.4. The subroutine is called by OVER and OVERLP.

MINA, an SNL mathematical program library subroutine, finds an approximate minimum of a real function identified by the first argument. The subroutine is called by CPQR and is used to identify the facet pulldown distance that maximizes the flux density at the focus point during canting (for facet shapes determined by stress analysis).

MLUSED, a replacement for an SNL mathematical program library subroutine, monitors usage of the library. The subroutine is called by several of the library routines. In HELIOS the routine immediately returns after a call.

NORF(J) calculates the unit vector VN(I=1 to 3,J) normal to facet J in the heliostat coordinate system. Present dimensions limit the number of facets to $1 \leq J \leq 25$. The subroutine is called by Program B and by Program C. The equations used are given as Eq 3.3-10 in Reference 1 (where the eta sub i should be replaced by n_i to agree with Figure 3-13).

NORM(F,WLIM,WNORM) normalizes the integral of a two-dimensional (2-D) probability-density function F between the radial limits 0 and WLIM. Azimuthal symmetry is assumed. The subroutine is called by Program D for sunshape normalization. WNORM is the normalization factor.

NORMC, which is identical to NORM and is called only by PHI in the overlay controlled by Program C, checks and possibly corrects normalization for the effective sunshape evaluated by NUCONV when a one-dimensional (1-D) effective sunshape is desired.

NUCONV(SIGEQ2,ECARR,ECXRR,ECYRR) provides the numerical convolution of the sunshape and the error cone. In the case of a 1-D error cone, SIGEQ2 is the square of the dispersion. A 2-D error cone is described by an elliptic

gaussian distribution with the angle ECARR between the u-axis and the ellipse axis with standard deviation ECXRR. The orthogonal axis of the ellipse has standard deviation ECYRR. The ellipse and angle ECARR appear in the u-v reflected-ray reference plane. The method and several examples of 2-D numerical convolutions are given in Reference 1, Sections 5.3.5 and 5.3.6. The subroutine is called by PHI.

ONECHK, an SNL mathematical program library subroutine, functions in error-message processing for other library subroutines. This subroutine is called by GAUS8 and QNC7.

ORTAR(VTAR,ITAR,ITARSH,XEXT,ZEXT,HE,HN,HZ,HL2,NOUT) calculates the VTAR for use in Subroutine TARGET to generate a rectangular target with dimensions XEXT by ZEXT, centered at coordinates VTAR(1,I), I=1,3 with its normal directed toward the heliostat positioned at HE,HN,HZ. ITAR and ITARSH are defined as 1 and 0, respectively. The subroutine is called by INDATA when ITARSH is input as 5 and when the first heliostat is processed.

OUTP provides a printed summary of most of the input variables for an individual HELIOS problem. The subroutine is called by Program A.

OVER(NSB,NHEST1,MAR,OX,OY,OZ,DAY) evaluates the shadowing (NSB=1) or blocking (NSB=2) for the heliostats being processed. NHEST1 is the number of heliostats (plus 1) for the blocking (shadowing) calculation. The additional "heliostat" is added to represent the shadow cast by the tower. The subroutine is called by SHBL. The flow diagram is given in Figure A-5.

OVERLP, which is very similar to Subroutine OVER, functions when each heliostat is tested for shadowing and blocking with all the other heliostats, rather than with only the set of nearest neighbors. This subroutine is called also by SHBL.

PHI(RL,VN,RB,VM) calculates the normalized (unit insolation, unit facet reflectivity) flux density at a given target point contributed by one of the elements of facet area. RL(I=1,3) gives the three components of the element center in the sun-concentrator coordinate system, VN(I=1,3) gives the facet normal, RB(I=1,3) gives the components of the target point, and VM(I=1,3) gives the unit normal to the target surface. The function PHI is called by function FACET.

PHI is within the innermost loop executed by the HELIOS Code. As a result, a gain in speed can substantially affect the cost of using the code. In some special applications users may want to alter the routine to meet their goal more economically. The flow diagram follows in Figure A-6. The routine evaluates the integrand in Eq 5.5-3 of Reference 1 for insolation $a=1$ and reflectivity $\rho=1$. The integrand is multiplied by the target absorption at the current value of $\cos \psi$.

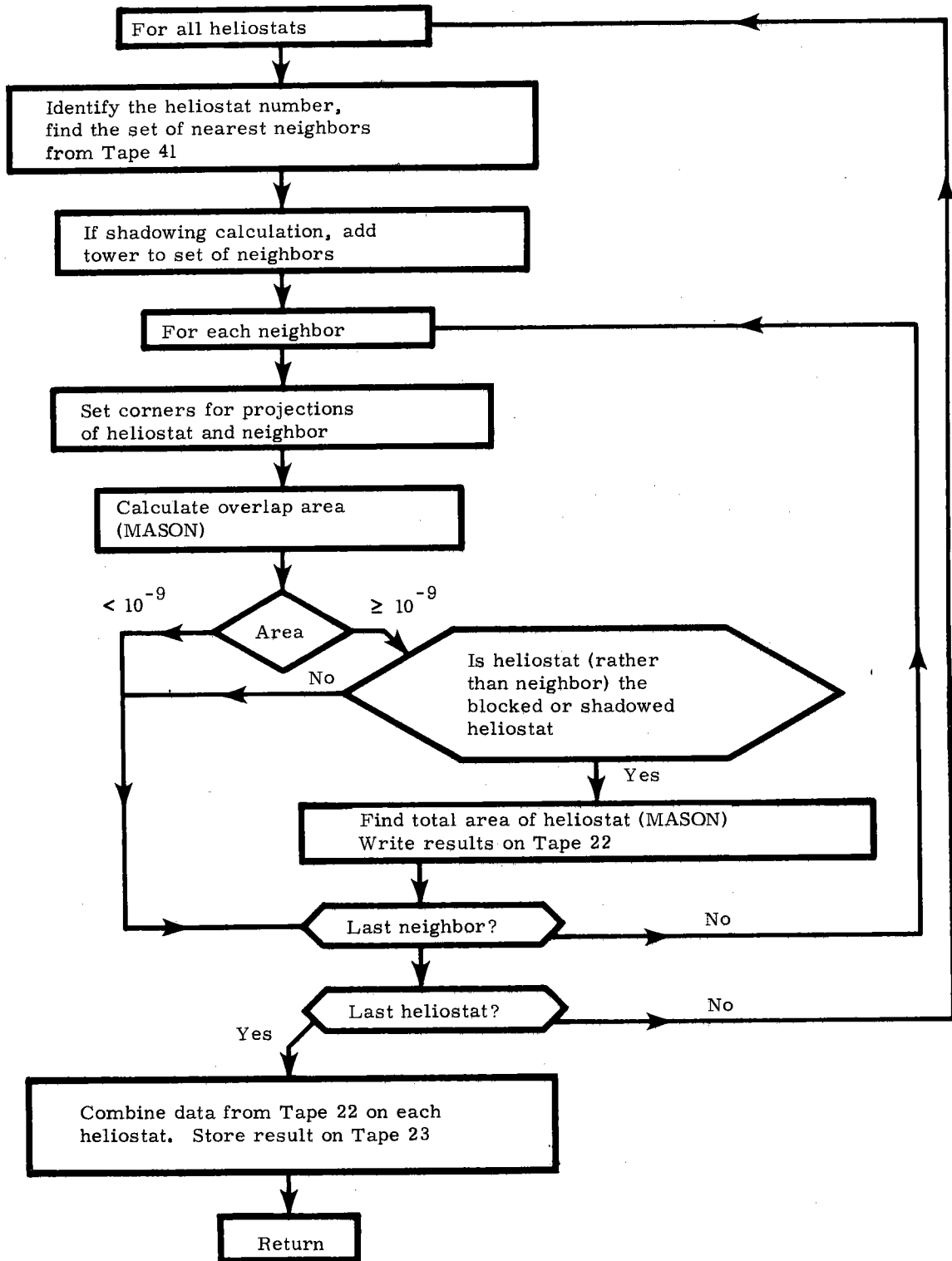
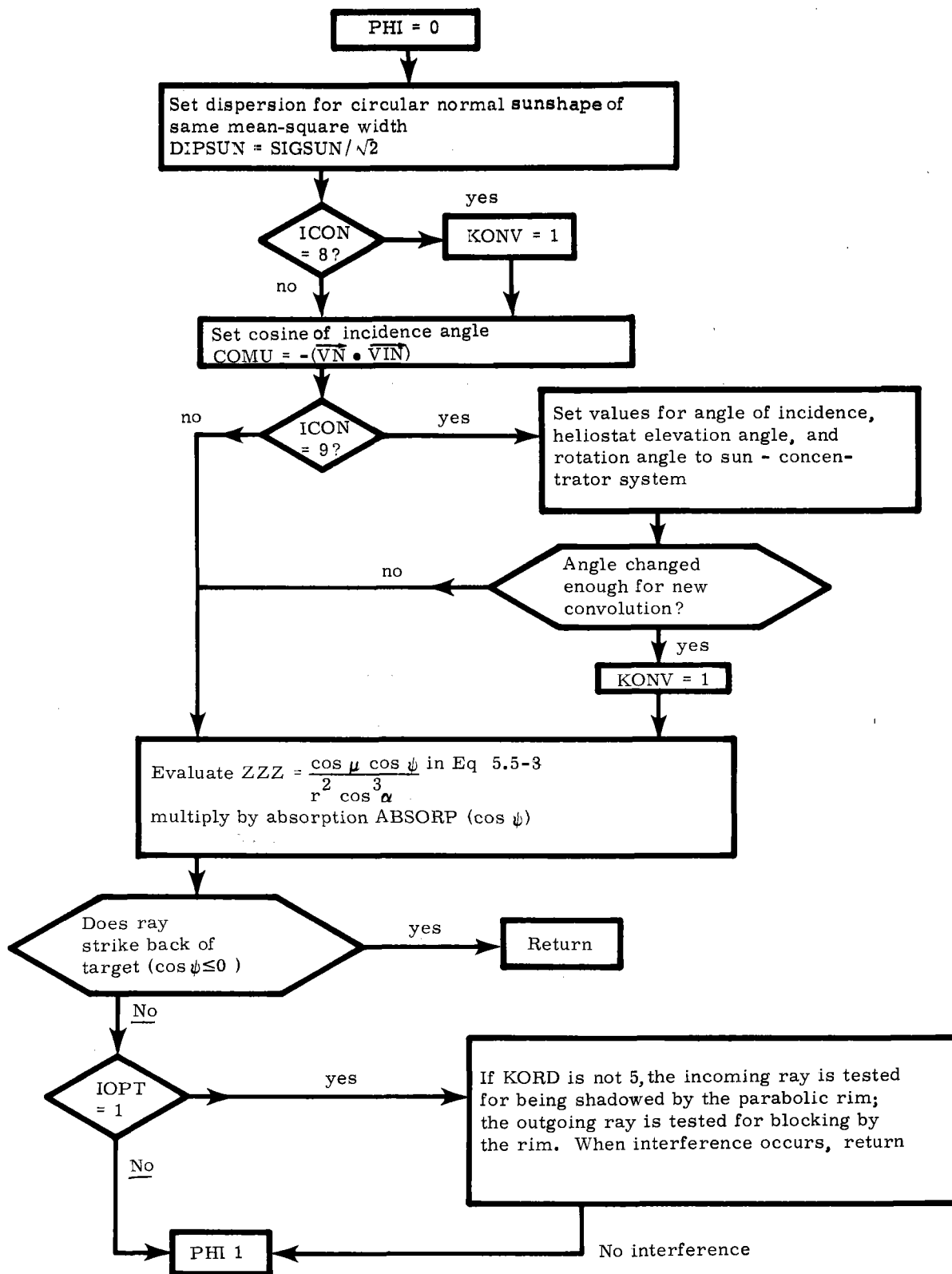


Figure A-5. Flow Diagram for OVER



Part A

Figure A-6. Flow Chart for PHI

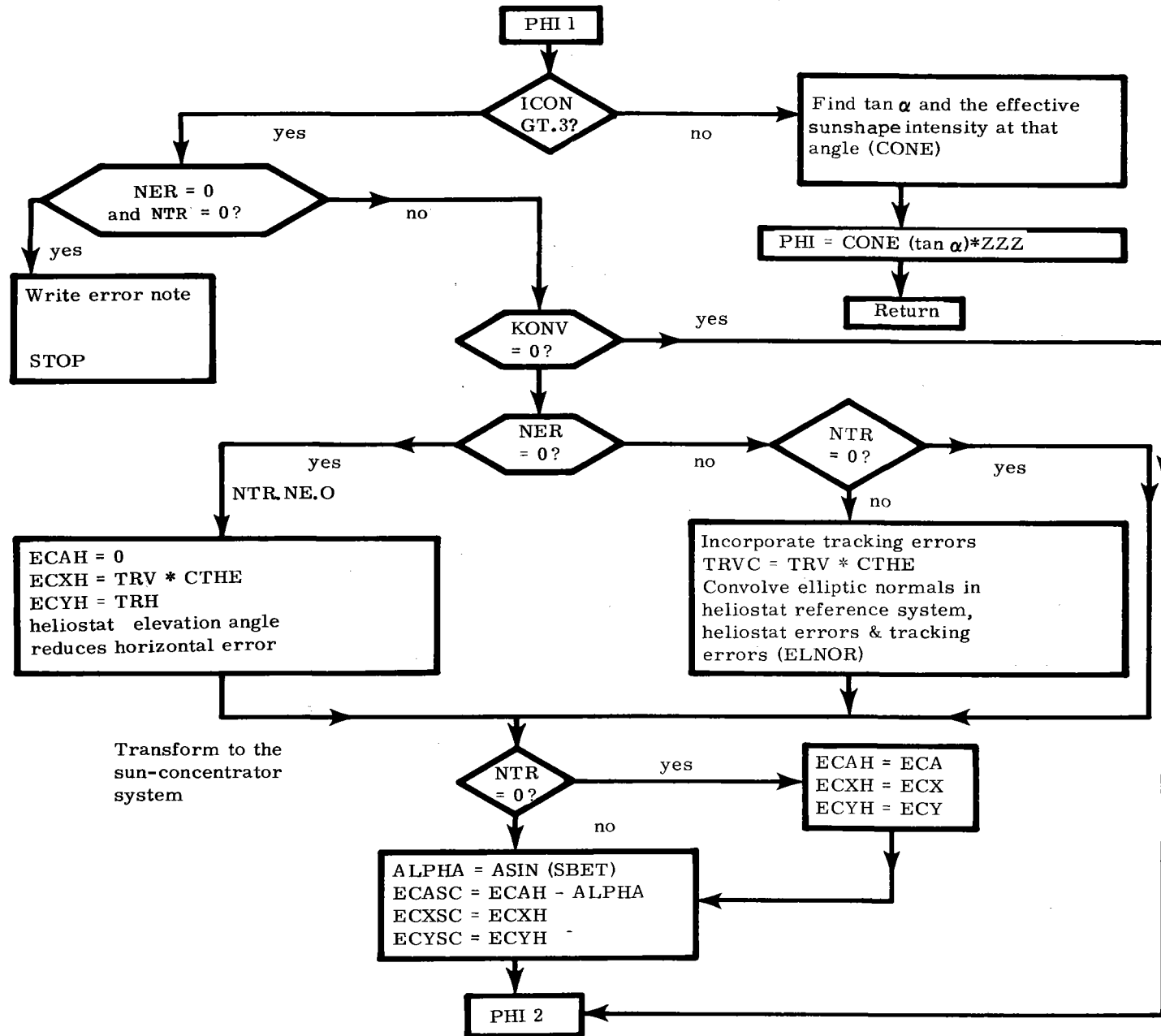
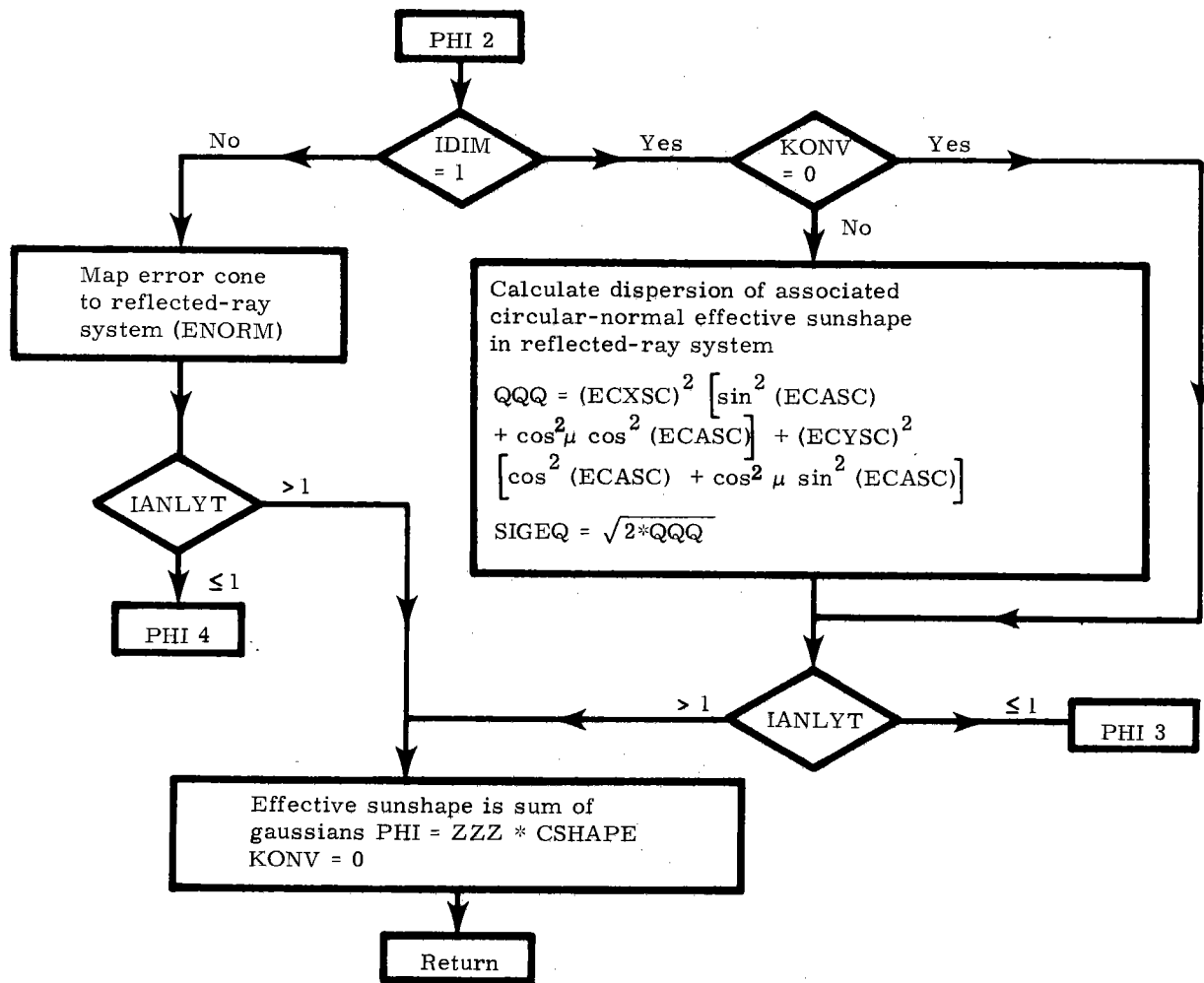


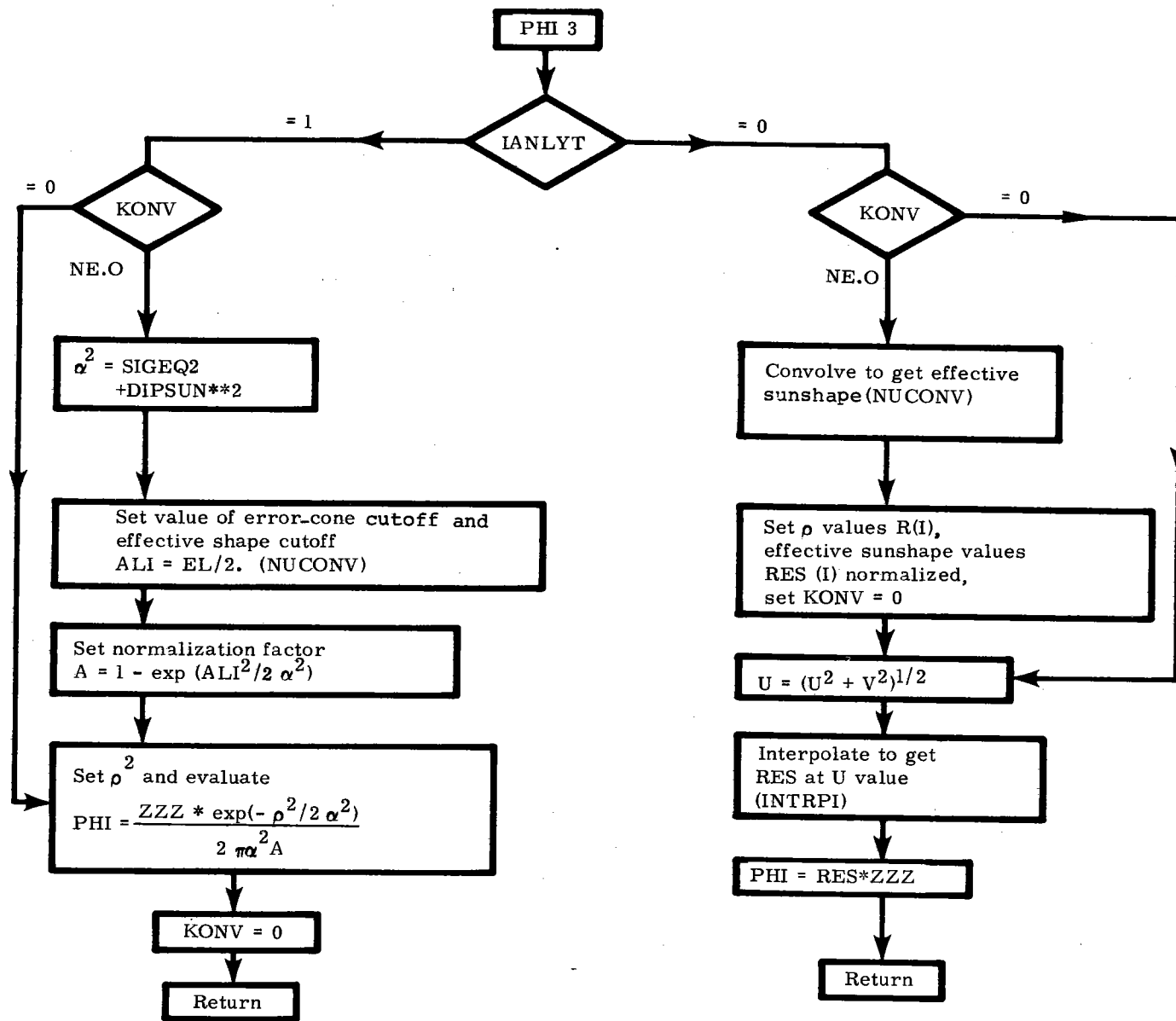
Figure A-6 (cont)

Part B



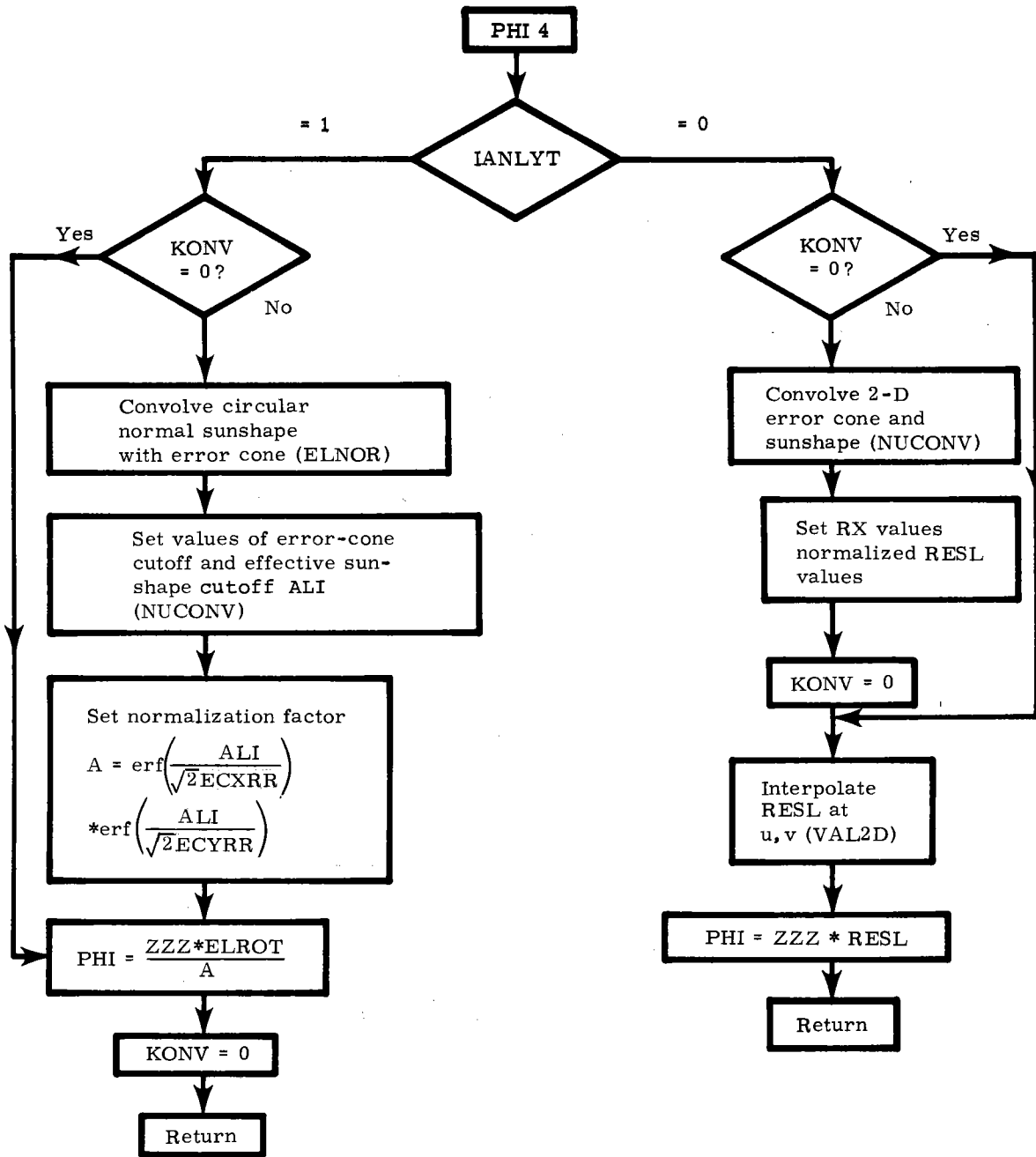
Part C

Figure A-6 (cont)



Part D

Figure A-6 (cont.)



Part F

Figure A-6 (concluded)

PHID, an abbreviated form of the function PHI, aids in determining the optimum pulldown distance when facet shape is determined by stress analysis. It is called from FACETA. A gaussian effective sunshape is used for rapid evaluation of the integrand in Eq 5.5-3 of Reference 1.

PLATE calculates the unit normal to the facet surface in the individual facet coordinate system as a function of position on the facet (RL(1),RL(2)). This subroutine is called from RVN when IOPT=3 or 4. PLATE was written by C. S. Hoyle of SNL at Livermore (SNLL).

POWERI(EFLUX, IXPTS, IYPTS, XM, YM, PIN) calculates the integral of the flux density over an 11-x-11 array of target points (IXPTS=11, IYPTS=11). The target coordinates of the points are XM(I), YM(I) for I=1,11. The EFLUX matrix gives the flux density at the 121 target points. The integral is returned as the power PIN. Weighting functions are used for the spherical or cylindrical target options. The method applies Eq 7.1-4b on p 143 of Reference 1. The subroutine is called by Program C to find the contribution from each separate heliostat, to find the power collected from each reconcentrator surface (when ITARSH=7), and to find the power collected directly and from reconcentrators (when ITARSH=7). The subroutine will likely require altering for user-generated target surfaces (ITARSH=2) or for IXPTS and IYPTS values other than 11.

POWREC(RECOP, IRECP, IXPTS, IYPTS, NOUT), a user-generated subroutine, integrates the flux-density incident upon each of the IRECP reconcentrator surfaces. Each reconcentrator surface has an IXPTS by IYPTS array of target points with flux densities stored in the matrix RECOP. NOUT is the tape drive for output; i.e., Tape 6. The subroutine is called by Program C when ITARSH=7. It must be altered whenever a new reconcentrating system is to be modeled.

PROP(D) calculates the propagation-loss factor appropriate for distance D metres. The function is called by Program C. Default input parameters cause evaluation of the loss factor by Eqs 6.3-2 and 6.3-3 on p 121 of Reference 1. Equation 6.3-3 for the percentage loss should read

$$L_s = 100[1. - \exp(-0.1852 R)]$$

for $0 \leq R < 0.1$ km, where R is D converted to kilometres. These formulae are limited to $R \leq 1$ km, site altitudes near 0.6 km above sea level (as for Barstow, California), and tower elevations from 0 to 300 m above the ground. Other formulae available are listed below. They are taken from Reference 7. The R values are always in kilometres.

The percentage propagation loss formulae appropriate for Barstow, California, at 0.61 km above sea level are:

At "sea-level visibility" 23 km,

$$L_{B23} = 0.6789 + 10.46 R - 1.70 R^2 + 0.2845 R^3 \quad 0.1 \leq R < 2 \text{ km}$$

$$L_{B23} = 100[1. - \exp(-0.1739 R)] \quad 0 \leq R < 0.1 \text{ km}$$

At "sea-level visibility" 5 km,

$$L_{B5} = 1.293 + 27.48 R - 3.394 R^2 \quad 0.1 \leq R \leq 2 \text{ km}$$

$$L_{B5} = 100[1. - \exp(-0.4090 R)] \quad 0 \leq R < 0.1 \text{ km}$$

The L_s for Barstow was generated in 1976. Its values are close to L_{B23} . However, the latter equation is thought more accurate for those atmospheric conditions.

Propagation loss formulae appropriate for Albuquerque, New Mexico, at 1.52 km above sea level are:

At "sea-level visibility" 23 km,

$$L_{A23} = 0.8090 + 6.04 R - 0.504 R^2 \quad 0.1 \leq R \leq 2 \text{ km}$$

$$L_{A23} = 100[1. - \exp(-0.1418 R)] \quad 0 \leq R < 0.1 \text{ km}$$

At "sea-level visibility" 5 km,

$$L_{A5} = 0.8986 + 13.78 R - 1.182 R^2 \quad 0.1 \leq R \leq 2 \text{ km}$$

$$L_{A5} = 100[1. - \exp(-0.2291 R)] \quad 0 \leq R < 0.1 \text{ km}$$

In Albuquerque a "sea-level visibility" 23 km corresponds to an Albuquerque visibility of about 60 km. These are the expected conditions during good weather. Visibility 5 km is sometimes referred to as a "hazy" day. The reference to sea level occurs because of the standard atmospheres chosen for evaluating the propagation loss. These atmospheres include density profiles making visibility vary with altitude.

The choice of formula is controlled by the loss-form parameter LFORM in Group 7 of the input data.

<u>LFORM</u>	<u>Formula</u>
0	L_s
1	L_{B23}
2	L_{B5}
3	L_{A23}
4	L_{A5}

QNC7, an SNL mathematical program library subroutine, integrates real functions of one variable over a finite interval. An adaptive 7-point Newton-Cotes algorithm is used. More details are available in Reference 3. The subroutine is called by Program D and by NORM, NORMC, and PHI. In each case a probability-density function is checked for proper normalization or else an rms width is calculated.

RANF, a random-number generator furnished as an intrinsic function in the CDC system, returns real values uniformly distributed over the range (0,1) with end points excluded. RANF is called by Subroutine JITTER in modeling the movement of heliostats within their encoder least-count.

RANSET, a utility subprogram furnished by CDC, initializes the seed used by Routine RANF.

RARE(NTAG,ISECT,RAREA) generates the ratio (RAREA) of an element of area on a reconcentrator to an element of area on the target. It is used only with ITARSH=7 and must be replaced when a new reconcentrating system is to be treated. The target point being treated is NTAG. The section of the reconcentrator is identified by ISECT. The subroutine is called only by Program C.

REF(NF,AMU) calculates the reflection coefficient for facet number NF at angle of incidence AMU. No wavelength dependence is presently included. The default reflection coefficient is set to 0.9 and can be changed by means of the input data. The function must be altered if angle-of-incidence variation is to be treated. REF is called by Program C.

RFBS,RLUD, SNL mathematical program library subroutines, solve a factored system of real linear algebraic equations and factor a system of such equations. They are called by the library Routine SAXB and discussed in Reference 3.

ROTAT($\delta, C, V1, V2$) rotates by δ radians about the axis defined by vector C from an old vector V1 to the new vector V2. The rotation axis C has direction cosines (C_1, C_2, C_3). The V2 is found by

$$\underline{V2} = A \underline{V1}$$

where the rotation matrix

$$A = \cos \delta \begin{pmatrix} 1 & 0 & 0 \\ 0 & 1 & 0 \\ 0 & 0 & 1 \end{pmatrix} + (1 - \cos \delta) \begin{pmatrix} C_1^2 & C_1 C_2 & C_1 C_3 \\ C_2 C_1 & C_2^2 & C_2 C_3 \\ C_3 C_1 & C_3 C_2 & C_3^2 \end{pmatrix} \\ + \sin \delta \begin{pmatrix} 0 & -C_3 & C_2 \\ C_3 & 0 & -C_1 \\ -C_2 & C_1 & 0 \end{pmatrix}$$

as indicated by Section 14.10-2 of Reference 4. Subroutine ROTAT is called by GETNSF.

ROTZ(cos β , sin β , RP, R) converts the components of vector RP in the facet coordinate system into the corresponding components of vector R in the sun-concentrator coordinate system. The β is the angle of rotation from the facet system to the sun-concentrator coordinate system. The subroutine is called from FACETA and FACET.

RVN(RL, VN) calculates the unit normal vector (VN) on the reconcentrator surface in the facet coordinate system as a function of the position on the reconcentrator designated by facet coordinates RL(1) and RL(2). The subroutine is called by FACETA, FACET, and INDATA.

SAXB, an SNL mathematical program library subroutine, solves a nonsingular system of real linear algebraic equations. It is called by CPQR in the process of canting the facets on a heliostat. Program C uses SAXB to find the target coordinates for intersection of the central reflected ray from a facet with the target plane. The routine is discussed in Reference 3.

SECOND, a CDC operating system interface routine, returns the central processor time (seconds) measured from the beginning of the job. This function is called by Programs A, B, C, D, and FOUR to provide relative timing information.

SHBL(DAY, TI, SV, XTCEN, YTCEN, ZTCEN) calculates the ratio of ineffective area (caused by shadowing or blocking) to total area for each heliostat at each day-of-year (DAY) and each time-of-day (TI) processed. The subroutine is called by Program B. The unit vector SV is directed from the heliostat center toward the sun. The XTCEN, YTCEN, ZTCEN are the tower coordinates of the target center and are used as the center of the unit sphere upon which the blocking is calculated. The methods used are discussed on pp 156-166 of Reference 1.

SMODN(X) calculates the smooth-down function describing the shape of the sunshape edge at $\tan \alpha = X$ for $1 \leq \text{JSUN} \leq 4$. The functional form is determined by the input parameter ID that is transferred by common block CLIMS. The function is called by CONE and CONEA.

SRATIO(SR) models the variation of solar insolation with atmospheric mass traversed. The atmospheric-mass-reduction factor is returned as the ratio SR. The subroutine is called by ELAZS. The equations used are discussed on pp 113-114 of Reference 1.

STEP(X,B), the unit step function, truncates probability-density distributions at the cutoff value B. The value 1 is returned for $X \leq B$. Otherwise 0 is returned. STEP is called by CONE, CONEA, and SMODN.

SUN(tan α ,SU) evaluates the sunshape when a bilinear interpolation scheme is used between data points input with JSUN=7. The intensity is returned as SU for value $\rho = \tan \alpha$. The subroutine is called by CONE and CONEA.

SUNPAR(NC,NSCAL,SCAL) uses the index NC to select coefficients for sunshape representation as a sum of gaussian distributions when IANLYT is 9, 7, 10, 6, or 16, giving successively wider sunshapes. NSCAL and SCAL are Group 2 input parameters that allow the coefficients to be scaled for a slightly different sunshape. The subroutine is called by INDATA. The method is discussed in Reference 8.

TARGET(NTAG,XTA,YTA,ZTA,VMT) calculates the tower coordinates XTA,YTA,ZTA, and the components of a unit vector normal to the target surface (VMT(I),I=1,3) for target point number NTAG. The subroutine is called by Program C and by INDATA. The methods used are discussed in Section 3.5 of Reference 1.

TCIRP calculates the tower coordinates of intersection with the target plane for a ray reflected from a reconcentrator. The subroutine is called by FACET when ITARSH=7. The method used is discussed in Section 8.1.1 of Reference 1.

TONE(X) calculates $X \cdot \text{CONE}(X)$ for use in Program D. This normalizes the effective sunshape when ICON=0, 2, or 3.

USERA(X) provides a gaussian probability-density function of $\rho = X$. Alteration and use of JSUN=5 allows the user to specify his own sunshape. The function is called by CONE and CONEA.

USERB(X) provides a uniform probability-density function of $\rho = X$. The function is called by CONE and CONEA when JSUN=6. In the present version of HELIOS, it is a duplication of the capability in JSUN=5 and USERA. Alteration will allow the user to specify the sunshape appropriate for light sources, either in nature or for laboratory measurements.

USERTG(NTAG,XTA,YTA,ZTA,VMT) functions as a means of user specification of tower coordinates XTA,YTA,ZTA and normal vector VMT(I)I=1,3 at target point number NTAG. The routine is called by TARGET when ITARSH=2. The present form describes the sections of the four panel reconcentrator discussed in Section 8.1.2 of Reference 1. In addition, a similar six-panel reconcentrator is also included in the subroutine.

USERVN(X,Y,VN) evaluates the unit vector (VN) normal to the facet surface at facet coordinates X,Y. The subroutine is called from RVN only when IOPT=7, where the user specifies his own facet shape. It is expected that the subroutine will be altered for most applications. In its present form the facets are given a cylindrical curvature along the facet x-axis. Although short, a flow diagram is included as Figure A-7 because of the high probability of alteration. The components are given in the facet coordinate systems where the x-axis is horizontal and tangent to the facet at its center, the z-axis is orthogonal to the facet at its center, and the y-axis completes the right-handed system. When altered, the user may also wish to change VALRL3.

VALRL3(RL) returns the third component RL(3) of the position on the facet (in the facet coordinate system) when the first two components, RL(1) and RL(2) are provided. The subroutine is called by FACET, FACETA, INDATA, and PHI.

VAL2D provides interpolation of a 2-D matrix representing a probability-density function. The subroutine is called by FU and by PHI when 2-D effective sun-shapes are used. The routine was written by R. E. Jones of SNLA's Computer Consulting and Training Division in November 1974.

VECCT calculates the tower coordinates of the facet-element center (VFE). The subroutine is called by FACET as it integrates over the elements of area on the facet. The basic equations used are 8.1-9 and 8.1-10 in Reference 1.

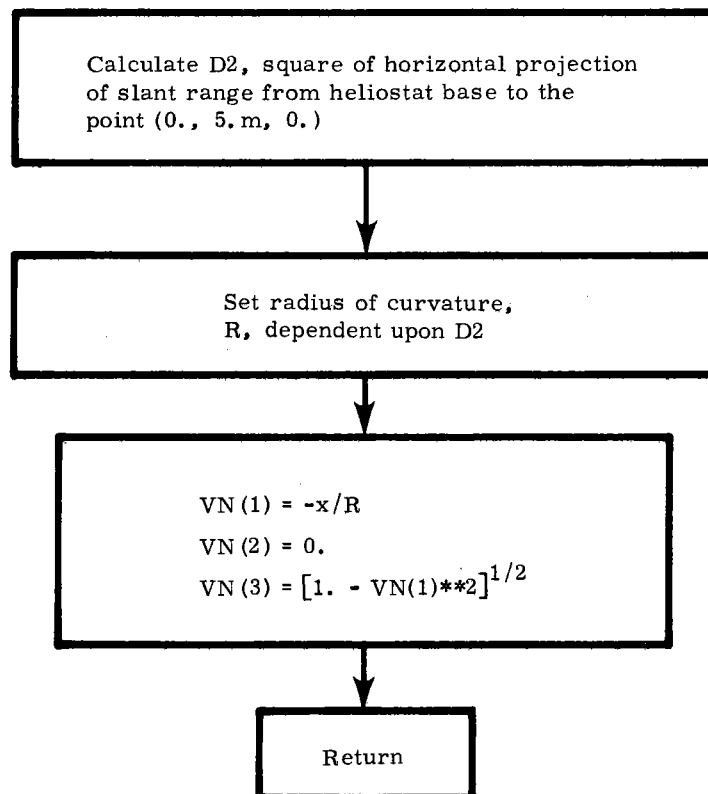


Figure A-7. Flow Diagram for USERVN

VNORT(IVMD,V) generates a vector V (in tower coordinates) that is roughly perpendicular to a plane target surface. The input parameter IVMD identifies the approximate direction of the normal. The subroutine is called by CONVU, which then orients the target coordinates as seen by an observer facing the target.

APPENDIX B
Input Variables

<u>Variable</u>	<u>Group</u>	<u>Routines Where Used*</u>	<u>Common Block Where Used</u>
AC(I,J)	3	APERT, APERTV	APER
AHI	2	OUTP, AUTSUN, D, FF, FPHONE, GG	CLIMS
ALO	2	OUTP, CONE, CONEA, D, FF, FPHONE, GG, AUTSUN	CLIMS
AZIMU	6	ELAZS	TIM
BET	2	OUTP, FF, GG, CONE, CONEA, D, FPHONE	STAT
BLIM	2	OUTP, FF, GG, AUTSUN, CONE, CONEA, D, FPHONE	CLIMS
BLIMG	2	D, GG, NUCONV	CGG
DAMAX	2	OUTP, PHI	TRKER
DEMAX	2	OUTP, PHI	TRKER
DFOC	6	A, OUTP	A3
DIMAX	2	OUTP, PHI	TRKER
EFWB	3	B, OUTP, SHBL	A2
EFWT	3	B, OUTP, SHBL	A2
ELCA	5	JITTER	LOCKER
ELCE	5	JITTER	LOCKER
ELENX	4	FACET, FACETA, SHBL	CKORD
ELENY	4	FACET, FACETA, SHBL	CKORD
ELEVA	6	ELAZS, GLOAD	TIM
EPSG	2	D, GG	CGG
EPSV	2	AUTSUN, C, D	MATERR
FEPSUN	2	OUTP	STAT
FLENG	4	HELIOS, OUTP (ELEN), CPQR (ELEN), FACET (ELEN), USERVN (ELEN), PHI	CFACET
G(I)	2	CSHAPE, D, SUNPAR	SPARAM
HDM(NH,J)	5		HEL
HE	5	A, AZELA, AZELB, B, C, JITTER, OUTP, ORTAR, USERVN, VALRL3, APADJ, FPAJ, ORTAR	A2
HEFOC	3	A, CPQR, FPAJ	FOCPT
HL1	5	OUTP, AZELA, AZELB, JITTER	A2
HL2	5	OUTP, AZELA, AZELB, C, JITTER, ORTAR	A2

<u>Variable</u>	<u>Group</u>	<u>Routines Where Used*</u>	<u>Common Block Where Used</u>
HN	5	A, OUTP, AZELA, AZELB, B, C, JITTER, USERNV, VALRL3, ORTAR, APADJ, FPADJ	A2
HNFOC	3	A, CPQR, FPADJ	FOCPT
HN(NH,I)	5	A, FOUR	BLANK, BCOM
HZ	5	A, OUTP, AZELA, AZELB, B, C, JITTER, FPADJ, ORTAR	A2
HZFOC	3	A, CPQR, FPADJ	FOCPT
IACCU	1	C, OUTP	A1
IANLYT	2	D, NUCONV, OUTP PHI	TRKER
IAPT	3	APERT, C, FACET, OUTP	APER
ICON	2	C, CONE, CONEA, D, HELIOS, OUTP, PHI	CONVOL
ICPQR	5	A, C, OUTP, CPQR	CFACET
ID	2	OUTP, SMODN, FF, GG, AUTSUN, D, FPHONE	CLIMS
IDIM	2	NUCONV, OUTP, PHI	TRKER
IGEO	3	C, OUTP	TARGET
IHELD	1	OUTP, A, B, C, HELIOS, OVER, OVERLP, SHBL	A1
INIT	2		
INSOL	2	OUTP, ELAZS	A1
INTERP	2	FI, D	TABLE
INVTR	3	C, OUTP	NVTR
IOPT	4	OUTP, CPQR, FACET, RVN, VALRL3, A, B, C, PHI, FOUR	COMRVN
IPL0T1	1	A, C, OUTP	A1
IPRINT	1	OUTP, AZELA, AZELB, ELAZS, CPQR, OVERLP, OVER, A, AUTSUN, B, C, FOUR, GLOAD, NUCONV, PHI, SUNPAR	A1
IPROP	1	C, OUTP	A1
IRECP	3	C, RARE, USERTG, POWREC	WINSTO
ISHAD	1	B, OUTP, OVERLP, OVER	A1
ISPHE	1	OUTP	ISP
ITAR	3	TARGET, OUTP, ORTAR	TARGET
ITARSH	3	C, COORD, TARGET, OUTP, FACETA, POWERI, ORTAR	AIMPT
IVMD	3	TARGET, OUTP, CONVU, VNORT	TARGET
IXPTS	3	COORD, TARGET, OUTP, RARE, POWERI, POWREC, C, USERTG	AIMPT
IYPTS	3	COORD, TARGET, OUTP, RARE, POWERI, POWREC, C, USERTG	AIMPT
I3	6		

<u>Variable</u>	<u>Group</u>	<u>Routines Where Used*</u>	<u>Common Block Where Used</u>
I5	4, 5		
I6	2, 4		
I7	3, 5		
JID	2	OUTP, SMODN, FF, GG, CONE, CONEA, D, FFONE, AUTSUN	CLIMS
JSUN	2	OUTP, FF, GG, CONE, CONEA, D, FFONE	STAT
KORD	4	B, C, OUTP, FACET, FACETA, PHI, OUTP	CKORD
LFORM	7	OUTP, PROP	ATMASS
LOCK	5	HELIOS, OUTP, AZELB, B, C	LOCKER
MVIAM	7	OUTP, SRATIO	ATMASS
NAI(I)	5		MAP
NAID	5	A, C	AIMBLO
NC1	4	B, OUTP	A1
NC2	4	B, OUTP	A1
NC3	4	B, OUTP	A1
NC4	4	B, OUTP	A1
NDY	6	HELIOS, OUTP, A, B, C, OVER, OVERLP	A3 or TIMED
NER	2	OUTP, PHI	TRKER
NFACET	4	OUTP, CPQR, A, B, C, FOUR, GETNSF	A1
NFACUD	4	FACET	CKORD
NFI(I)	5		MAP
NFID	5	A	AIMBLO
NFOC	3	A, OUTP	FOCPT
NGL	4	C, OUTP	GRAVLD
NGRUP	ALL		
NHELI	5	OUTP, SHBL, OVERLP, OVER, A, AZELA, AZELB, B, C, CPQR, APADJ, FPADJ	A1
NHEST	5	OUTP, SHBL, OVERLP, OVER, A, B, C, FOUR	A1
NPOIT	3	OUTP	AIMBLO
NSCAL	2	SUNPAR	
NSUBF	4	OUTP	CKORD
NTABL	2	SUN	SUNTAB
NTARST	3	C, OUTP	NVTR
NTART	3	C, TARGET, OUTP	AIMPT
NTD	6	HELIOS, OUTP, A, B, C	A3
NTLOCK	5	HELIOS, AZELB, B, C, OUTP	LOCKER

<u>Variable</u>	<u>Group</u>	<u>Routines Where Used*</u>	<u>Common Block Where Used</u>
NTR	2	OUTP, PHI	TRKER
NUD	4	FACET	CKORD
NX	4	FACET, FACETA	CKORD
NY	4	FACET, FACETA	CKORD
P	7	OUTP, ELAZS, SRATIO	ATMASS
PHIL	3	C, OUTP	A1
PN	5	A, B, C, NORF, CPQR, FOUR	CFACET
PO	7	OUTP, ELAZS, SRATIO	ATMASS
POIS	4	RVN, OUTP	HOYLE
QN	5	A, B, C, NORF, CPQR, FOUR	CFACET
REFLEC	4	OUTP, REF	REFL
RHOLE	4	FACET, OUTP	RHOL
RN	5	A, B, C, NORF, CPQR, FOUR	CFACET
RNAUT	4	RVN, OUTP	HOYLE
S	2	ELAZS, AUTSUN, C	ATMASS
SCAL	2	SUNPAR	
SIGX(I)	2	OUTP, ELNOR, ELROT	TRKER
SIGY(I)	2	OUTP, ELNOR, ELROT	TRKER
SLEWRV	5	AZELA, AZELB, OUTP	SLEW
TD(I)	6	HELIOS, OUTP, AZELA, AZELB	A3
TEMP	7	OUTP	ATMASS
TFOC	6	A, OUTP	A3
TH(I)	2	OUTP	TRKER
TRH	2	OUTP, PHI	TRKER
TRV	2	OUTP, PHI	TRKER
TY(I)	6	HELIOS, OUTP, DECSUN(DAY)	A3
U	7	OUTP, SRATIO	ATMASS
U1(I)	4	A, B, C, CPQR, HELIOS, FOUR	PQR
U2(I)	4	A, B, C, CPQR, HELIOS, FOUR	PQR
U3(I)	4	A, B, C, CPQR, HELIOS, FOUR	PQR
VTAR(I,J)	3	HELIOS, COORD, TARGET, OUTP, CONVU, C, POWERI, ORTAR	TARGET
W	7	SRATIO	ATMASS
XEXT	3	HELIOS, TARGET, OUTP, C, ORTAR	TARGET
XFOC(I)	3	A, OUTP	FOCPT

<u>Variable</u>	<u>Group</u>	<u>Routines Where Used*</u>	<u>Common Block Where Used</u>
XPOIT	3	AZEL(XAIM), AIM	POINT
XPOT(I)	3	A, OUTP	AIMBLO
XTL	2	SUN	SUNTAB
YFOC(I)	3	A, OUTP	FOCPT
YPOIT	3	AZEL(YAIM), AIM	POINT
YPOT(I)	3	A, OUTP	AIMBLO
YTL	2	SUN	SUNTAB
ZEF	3	B, OUTP, SHBL	A2
ZEXT	3	HELIOS, TARGET, OUTP, C, USERTG, ORTAR	TARGET
ZFOC(I)	3	A, OUTP	FOCPT
ZPOIT	3	AZEL(ZAIM), AIM	POINT
ZPOT(I)	3	A, OUTP	AIMBLO
ZT	3	OUTP, B	A2

*All are listed in INDATA (not listed); most are in DATA1 (also not listed).

APPENDIX C

HELIOS Common-Block Connections

HELIOS has been constructed with many subroutines to aid the user in identifying specific tasks and, when necessary, in altering the method employed. Since creation of the code in the early months of 1976, there has been a continuing series of alterations and additions. This experience has taught us to exercise caution in making alterations for fear of disturbing sections already in operation. We found that a listing of the subroutine and common-block connections between various components in HELIOS aided the user in making alterations without disturbing other sections of the code. Such lists are conveniently generated at Sandia by use of an undocumented computer code developed by Larry Dike of Dikewood, Inc, Albuquerque, New Mexico. Results of this code applied to HELIOS follow here in Appendix C and also in Appendix E. Concentrated effort could probably improve the organization and efficiency of HELIOS as well as reduce the number of subroutines and common blocks. However, present demands of highest priority are aimed at additional capabilities and use rather than code refinement. This appendix gives the interconnections for common blocks, while Appendix E treats the routines themselves.

<u>Common Block</u>	<u>Routines Where Used</u>
AIMBLO	A, DATA1, INDATA, OUTP
AIMPT	HELIOS, TARGET, INDATA, OUTP, DATA1, AZELA, AZELB, FACET, FACETA, POWERI, A, B, C, USERTG, PHI
ANGDST	C, DATA1, HELIOS
AONE	B, SHBL
APER	APERT, APERTV, C, DATA1, FACET, HELIOS, INDATA, OUTP
ATMASS	HELIOS, INDATA, OUTP, DATA1, ELAZS, ATM, AUTSUN, SRATIO, C, PROP
ATWO	B, C, HELIOS
A1	HELIOS, TARGET, INDATA, OUTP, DATA1, AZELA, AZELB, ELAZS, CPQR, ATM, RVN, SHBL, OVERLP, OVER, PHI, PROP, A, APERT, AUTSUN, B, C, CONV, D, FACET, FACETA, FOUR, GETNSF, GLOAD, JITTER, NUCONV, SUNPAR, USERTG
A2	HELIOS, INDATA, OUTP, DATA1, AZELA, AZELB, CPQR, A, B, C, JITTER, SHBL, USERVN, VALRL3
A3	HELIOS, INDATA, OUTP, DATA1, AZELA, AZELB, OVERLP, OVER, A, B, C
A4	HELIOS, INDATA, OUTP, DATA1, AZELA, AZELB, ELAZS, ATM, USERA, A, B, C, D, ELNOR, ELROT, ENORM, GLOAD, JITTER, NUCONV, PHI, CSHAPE
A5	HELIOS, AZELA, AZELB, ELAZS, NORF, CPQR, A, B, C, JITTER, PHI
BCOM	C, FOUR
CEEED	HELIOS, INDATA, USERVN, VALRL3

<u>Common Block</u>	<u>Routines Where Used</u>
CELL	A, B, C, DATA1, HELIOS, INDATA, OUTP, OVER, SHBL
CENTAR	B, C, DATA1, HELIOS, INDATA
CENTER	C, HELIOS
CFACET	A, B, C, CPQR, DATA1, HELIOS, INDATA, NORF, OUTP, PHI
CFF	INDATA, FF, D, DATA1, FFONE, HELIOS, NUCONV
CGG	INDATA, GG, D, HELIOS
CKORD	HELIOS, INDATA, OUTP, DATA1, CPQR, FACET, USRVN, B, C, FACETA, PHI, SHBL
CLIMS	HELIOS, INDATA, OUTP, DATA1, SMODN, FF, GG, CONE, AUTSUN, CONEA, D, FFONE
COMFOC	HELIOS, RVN, VALRL3, C
COMPFI	HELIOS, CPQR, PHI, PHID, C
COMRVN	HELIOS, INDATA, OUTP, DATA1, CPQR, FACET, RVN, VALRL3, PHI, A, B, C, FACETA
CONVOL	INDATA, DATA1, CONE, C, CONEA, D, HELIOS, OUTP, PHI
FACOLE	FACET, RVN, FACETA
FOCPT	HELIOS, INDATA, OUTP, DATA1, CPQR, A
FVU	FU, FV
GRAVLD	C, DATA1, HELIOS, INDATA, OUTP
HEL	INDATA
HOYLE	HELIOS, INDATA, OUTP, DATA1, CPQR, RVN, FN, C
ISP	INDATA, DATA1, OUTP
LOCKER	HELIOS, INDATA, OUTP, DATA1, AZELB, B, C, JITTER
LONE	C, HELIOS, PHI
MAP	A, INDATA
MATERR	HELIOS, INDATA, DATA1, AUTSUN, C, D
NVTR	HELIOS, INDATA, OUTP, DATA1, C
NWRAYS	C, FACET
OPT	HELIOS, CPQR, FN, C
PHFF	FRES, FU, FV, PHI, HELIOS, NUCONV
POINT	INDATA, OUTP, DATA1, AIM, HELIOS
POWTOT	C, HELIOS
PQR	HELIOS, INDATA, OUTP, DATA1, CPQR, A, B, C
PU	A, CPQR
RECON	C, FACET, PHI
REFL	INDATA, OUTP, DATA1, REF, HELIOS
REFRA	INDATA, OUTP, DATA1, ELAZS, HELIOS, JITTER

<u>Common Block</u>	<u>Routines Where Used</u>
RHOL	DATA1, FACET, HELIOS, INDATA, OUTP
SLEW	HELIOS, INDATA, AZELA, AZELB, B, C, DATA1, OUTP
SPARAM	CSHAPE, D, HELIOS, INDATA, SUNPAR
STAT	HELIOS, INDATA, OUTP, FF, GG, CONE, CONEA, A, AUTSUN, C, D, DATA1, FPHONE
SUN	HELIOS, DECSUN, ELAZS, A, B, C, JITTER
SUNAIM	B, C, HELIOS, INDATA
SUNTAB	INDATA, SUN, D, HELIOS
SUN2	HELIOS, PHI
TABLE	INDATA, FI, CONV, D, HELIOS
TARGET	HELIOS, TARGET, INDATA, OUTP, DATA1, C, CONVU, POWERI, USERTG
TARXY	HELIOS, TARGET, C
TIM	ELAZS, INDATA, HELIOS
TIMED	SHBL, OVERLP, OVER
TRITST	C, FACET, PHI
TRKER	HELIOS, INDATA, NUCONV, OUTP, PHI, D
USER	INDATA, USERA, D, HELIOS
WINSTO	C, DATA1, FACET, HELIOS, INDATA, RARE, USERTG
BLANK	A, C, CONV, D, INDATA

APPENDIX D

HELIOS Common-Block Parameter Lists

The HELIOS Code has evolved in a series of quantum jumps as new capabilities were added to deal with new geometries or furnish greater detail about the old ones. More often than not, the sense of urgency in the change meant a specific problem could be solved. One casualty of this approach is some lack of agreement between the 65 common blocks as they appear in various subroutines and functions. As an example, the ATMASS common block in Subroutine INDATA uses P to represent the air pressure, while in function PROP the pressure is represented by PRES. In PROP the P represents another variable. Here we list each common block and indicate at least one meaning for each of its variables. Although the name may change within some routines, the meaning remains for variables in the same sequential order. Comment statements within the code should aid in those few cases where variable meanings are altered inside certain routines. A future version of HELIOS may remove the need for such warnings, but they must be included at present lest the user become more trusting than he should.

Common Block	Parameter List
/AIMBLO/	<p>Heliostat aiming--strategy block</p> <p>NAID - index for aim point</p> <p>XPOT } array of tower coordinates for up to 222 different aim YPOT } points ZPOT }</p> <p>NPOIT - number of aim points</p> <p>NFID - index of prealignment point ,</p>
/AIMPT/	<p>Target specification block</p> <p>XAIM } YAIM } tower coordinates of current value of aim point ZAIM }</p> <p>NTART - number of target points on target or reconcentrator</p> <p>IXPTS - number of target points along row</p> <p>IYPTS - number of target points along column</p> <p>ITARSH - receiver shape index</p> <p>NTARSH - subtarget option index</p> <p>NTZV - index specifying subtarget number</p>

/ANGDST/ Flux-density angular distribution block

THEMIN } limits for cosine of polar angle
 THEMAY }
 DTHETA - interval of cosine for tabulation
 PHIMIN - minimum azimuthal angle
 DPHI - azimuthal angle interval for tabulation
 IMAX - number of polar angle intervals
 JMAX - number of azimuthal angle intervals
 PHISAT - array of azimuthal angles tabulated
 PACOS - array of polar angle cosines tabulated

/AONE/ Shadowing and blocking preparation block

OX } array of tower coordinates for four corners of heliostats
 OY } within one cell
 OZ }
 MAR - array of heliostat identification numbers

/APER/ Aperture parameter block

IAPT - aperture type index
 V41 } components of vectors between indicated corners of aperture
 V12 }
 AC - array of coordinates defining aperture
 U12 } unit vectors in direction of V12 and V41
 U41 }
 HXL } 1/2 of horizontal and vertical extents of aperture
 HYL }

/ATMASS/ Atmospheric parameter block

ELV } array of elevation angle and corresponding relative
 VMASS } atmospheric mass
 ATMA - present value of relative atmospheric mass
 PO - reference air pressure (1 atm)
 P - air pressure
 SO - insolation above atmosphere (0.1353 W/cm^2)
 S - insolation (W/cm^2)
 TEMP - air temperature ($^{\circ}\text{C}$)
 MVIAM - index for insolation model
 U - insolation model parameter
 W - precipitable water overhead (mm)
 LFORM - transmission loss index

Common Block

Parameter List

/ATWO/

Shadowing and blocking block

SBM - array of shadowing and blocking factors for the heliostats within one cell

/A1/

Group 1 and general block

NTAPE - input tape number, 5

NOUT - output tape number, 6

PHIL

CPHIL } site latitude along with cosine and sine

SPHIL }

IPRINT - print index

IPLOTI - PLO plot index, 0 or 40

NFACET - number of facets per heliostat

NHELI - heliostat identification number

NHEST - number of heliostats in cell

ISHAD - shadowing and blocking index

IACCU - calculation detail index

INSOL - solar insolation index

NC1

NC2 } facet numbers at corners

NC3 }

NC4 }

IHELD - heliostat insertion index

IPROP - transmission loss index

NEIGH - nearest neighbor parameter

/A2/

Heliostat and tower parameter block

HE } tower coordinates of base center for heliostat being

HN } processed

HZ }

HL1 } heliostat design parameters

HL2 }

ZT - tower height (used only for default target)

ZTEST } angle convergence test parameters for heliostat aiming

PTEST }

ZEF - effective tower height for shadowing

EFWT } effective radius of tower at top and bottom for shadowing

EFWB } calculation

/A3/

Time block

NDY - number of days to be included in calculation

NTD - number of times of day

Common Block

Parameter List

TY - day of year array
 TD - time of day array
 DFOC - prealignment (focusing or canting) day
 TFOC - prealignment time

/A4/ Mathematical constant block

PI - π
 PIRAD - $\pi/180.$
 PID2 - $\pi/2.$

/A5/ Orientation block

CZETAS - cosine sun elevation angle
 CPHIS - cosine sun azimuthal angle
 CZET - cosine aim point elevation angle
 CPHIT - cosine aim point azimuthal angle
 SPHIS - sine sun azimuthal angle
 SPHIT - sine aim point azimuthal angle
 ZETAT - elevation angle for aim point
 PHIT - azimuthal angle for aim point
 X1
 Y1 } tower coordinates of center for facet being processed
 Z1 }
 THE - heliostat elevation angle
 CTHE - cosine THE
 STHE - sine THE
 CPHIH } cosine and sine of heliostat azimuthal angle
 SPHIH }
 SZETAS - sine sun elevation angle
 ETA1 } components of unit vector normal to heliostat, in tower
 ETA2 } coordinates
 ETA3 }

/BCOM/ Program FOUR-C common block

HNM - array of heliostat identification numbers assigned
 X
 Y } array of tower coordinates for heliostat bases
 Z }
 MAR - array of input heliostat identification numbers

The above variables appear in Program FOUR. The variable below occurs only in Program C. Both sets of variables are listed in common blocks only because in some applications they may be assigned to LEVEL 2 and a labeled common block would be required.

Common Block

Parameter List

B - array of incident brightness at each target point for series of intervals of polar and azimuthal angle.
Parameter is used only when IGEO=3

/CEEBD/ Focal boundary block

B - array of boundary distances at which heliostat focal length changes when default version of USERVN is used and when IOPT=7

/CELL/ Cell parameter block for IHELD=2

NCELLS - number of cells
NHESC - number of heliostats in cell being processed
NCEL - index for cell being processed
NCELL1 - index for first cell that contains heliostats on Tape 3

/CENTAR/ Heliostat blocking-center coordinate block

XTCEN } tower coordinates of center of unit sphere used for
YTCEN } blocking calculations
ZTCEN }

/CENTER/ Target-center coordinate block

CNX }
CNY } tower coordinates for target center
CNZ }

/CFACET/ Facet alignment block

PN } array of facet normals in the heliostat coordinate system
QN } for heliostat being processed
RN }

ICPQR - prealignment-method index
VN - array of facet normals in the tower coordinate system for the heliostat being processed
FLENG - facet length parameter

/CFF/ Kuiper sunshape and limb-darkening block

FMUL - sunshape normalization parameter
JSUNF - sunshape parameter JSUN
DELF - sunshape parameter EPSUN
EPSF - parameter no longer used
BETF - sunshape parameter BET

ALOF - sunshape parameter ALO
 AHIF - sunshape parameter AHI
 IDF - sunshape parameter ID
 JIDF - sunshape parameter JID
 BLIMF - sunshape parameter BLIM

/CGG/

Error-cone shape block

GMUL - error-cone normalization parameter
 JSUNG - set to 2 for gaussian error cone
 DELG - set to 0, no longer used
 EPSG - error-cone dispersion parameter
 BETG - error-cone parameter no longer used
 ALOGG } tangents of angles for error-cone tail limits, BLIMG=0.001
 AHIG } and BLIMG.
 IDG - set to 3 for linear decay of error cone between ALOGG and
 AHIG
 JIDG - error-cone decay parameter set to 1
 BLIMG - error-cone cutoff parameter

/CKORD/

Facet shape block

KORD - shape index
 ELEN - length parameter
 NSUBF - subdivision index for integration over facet
 CBET } cosine and sine of facet orientation angle in Program C
 SBET }
 ELENX } horizontal and orthogonal lengths for rectangular facets
 ELENY }
 NX } number of horizontal and orthogonal subdivisions for facet
 NY } integration with rectangular facets
 NUD - number of triangular facets with horizontal edge upward
 NFACUD - array of triangular facet numbers with horizontal edge
 upward

/CLIMS/

Shape parameters for sunshape or error cone. The parameters are set elsewhere, such as in FF or GG and used in CONEA or CONE.

ALO } These parameters are set to those with an F suffix listed
 AHI } under common block CFF or set to those with a G (or GG)
 ID } suffix listed under common block CGG.
 JID }
 ZNORM - distribution normalization parameter
 BLIM - cutoff parameter for sunshape or error cone

Common Block

Parameter List

/COMFOC/ Facet curvature block

FOC - focal length when facet shape parabolic
R - radius of curvature when facet shape spherical

/COMPHI/ Incident-ray block

VIN - components of unit vector in sun-concentrator system in direction of incident ray

/COMRVN/ Facet surface-shape block

IOPT - facet shape index

/CONVOL/ Effective sunshape convolution-method block

ICON - effective sunshape convolution parameter
EPSQ - effective sunshape dispersion when ICON=2
SIGSUN } root-mean-square width and its square for the sunshape
SINSN2 }

/FACOLE/ Hoyle length parameter block

EL - 0.5 x length of square facet edge or radius of circular facet. The parameter is used with the Hoyle options (IOPT=3 or 4)

/FOCPT/ Heliostat prealignment block

HEFOC } tower coordinates of prealignment aim point for heliostat
HNFOC } being processed
HZFOC }

NFOC - number of prealignment aim points
XFOC } array of tower coordinates for all heliostat prealignment
YFOC } aim points
ZFOC }

/FVU/ Effective sunshape interpolation block

Z - tangent of view angle at which amplitude is sought for 2-D effective sunshape. Parameter used in FU and FV

/GRAVLD/ Gravity loading index block

NGL - gravity- or wind-loading index

Common Block

Parameter List

/HEL/ CRTF heliostat base coordinate block

HDM - array of tower coordinates for heliostat bases used when IHELD is 0 or 1. A common block is used so data statements can store the coordinates for the CRTF

/HOYLE/ Hoyle facet-parameter block

RNAUT - radius of center support for adjusting focus

CD - pulldown distance varied in CPQR to maximize power received at prealignment point

POIS - Poisson ratio for facet material

/ISP/ Special data-flow parameter block

ISPHE - Group 1 input parameter, used to control input-data flow

/LOCKER/ Heliostat position locking block

LOCK } lock option indices in Group 5 data set

NTLOCK }

JITT - heliostat jitter option index

ELCE } encoder least counts for elevation and azimuthal angle (in

ELCA } radians)

/LONE/ Effective sunshape block

KONV - parameter indicating need for new effective sunshape convolution

AIOLD } ICON=9 parameters indicating need for new effective

AEOLD } sunshape

AAOLD }

ESA } parameters describing 2-D elliptic normal effective

ESX } sunshape

ESY }

SIGEQ2 - square of SIGEQ

COSESA } cosine and sine of ESA

SINESA }

SIGEQ - dispersion for 1-D gaussian effective sunshape

/MAP/ Heliostat aiming-index block

NFI } array of prealignment-point and aim-point indices for up

NAI } to 559 heliostats read in with Group 5 data when IHELD=1

Common Block

Parameter List

/MATERR/

Error-cone dispersion block

EPSV - dispersion for error cone when ICON=0 or 3

/NVTR/

Target print-interval block

NTARST - starting target-point index giving printout for each facet when IPRINT=2

INVTR - interval between target points where facet printout occurs

/NWRAYS/

Reconcentrator-ray block

NWRC - array indicating number of cone-optics rays striking target points on each reconcentrator section

NWRE - array indicating number of cone-optics rays contributing to sections of target tabulated as function of reconcentrator section

IBASX } indices indicating section of target a cone-optics ray
IBASY } contributes to after reflection from a reconcentrator section

RAREA - ratio of area for reconcentrator area element to area for receiver element

NRS - array indicating number of cone-optics rays contributing directly to each target point

NRSTI - target point index in C and FACET

/OPT/

Sun-concentrator system block

RB - three coordinates of the target point in the sun-concentrator coordinate system

VM - three components of unit vector perpendicular to the target surface at the target point in the sun-concentrator coordinate system

/PHFF/

Sunshape interpolation block

RSET - array of tangents for 1-D sunshape tabulation

RX - array of tangents for 2-D sunshape tabulation

ALIM - cutoff value for 2-D sunshape tabulation

ELI - cutoff value for 1-D sunshape tabulation

RES - array of sunshape amplitudes for 1-D sunshape interpolation

RESL - array of sunshape amplitudes for 2-D sunshape interpolation

/POINT/ Aim block

XPOIT } tower coordinates of a point toward which the heliostats
 YPOIT } are aimed when NPOIT=1. They also specify the center of
 ZPOIT } the target mesh when ITAR=0

/POWTOT/ Subtarget block

PSAV - sum of power collected by a series of subtargets. Used
 when $9 < \text{ITARSH} < 17$

/PQR/ Facet orientation block

U1 } array of coordinates for facet centers in heliostat
 U2 } coordinate system
 U3 }

AF - array of facet areas for all facets on a heliostat
 RF - array of 2 x focal length for spherical or parabolic
 facets on heliostat being processed
 SL - array of length parameters for all facets of heliostat
 being processed
 FOCM - array of focal lengths for spherical or parabolic facets
 on heliostat being processed
 CDM - array of pulldown distances for each facet center on
 heliostat being processed with IOPT=3 or 4. The array is
 set in CPQR

/PU/ Facet-normal punch block

NPUNCH - set to 8 in Program A to define tape number for
 punched-card output

/RECON/ Reconcentrator block

VX } components of 3 unit vectors in tower coordinates pointing
 VY } in direction of axes in the facet coordinate system
 VZ }

XIP } tower coordinates of the facet center
 YIP }
 ZIP }

VMT - three components of unit normal to surface at target point
 being processed

XTA } tower coordinates of target point being processed. The
 YTA } point may be on a reconcentrator surface when $\text{IRECP} > 0$
 ZTA } and $\text{ITARSH}=7$

NTAG1 - target point index

Common Block

Parameter List

XTO } target-point coordinates for target center. Used when
YTO } reconcentrators are being processed
ZTO }

BASK - array of flux density contributed at each target point
tabulated separately for each reconcentrator reflector

RECN - unit normal to reconcentrator section at reflection point

BASKM - parameter defined in Program C as an aid to obtaining flux
density at a target point in C and in evaluating BASK in
FACET

/REFL/ Reflectivity block

REFLEC - facet reflectivity

/REFRA/ Refraction block

AEL - array of apparent elevation angles for sun

TEL - corresponding array of true elevation angles for sun

TMAT - array of differences AEL-TEL defined in DATA1

/RHOL/ Facet hole block

RHOLE - radius of hole in center of circular facet when KORD=4

/SLEW/ Slue block

SLEWRV - slue rate in rad/h

NT - index for time loop in HELIOS

/SPARAM/ Summation gaussian sunshape block

G - array of coefficients describing sunshape as sum of
gaussians. Built-in sets are listed in SUNPAR

/STAT/ Sunshape parameter block

JSUN - sunshape index

EPSUN - tangent of (FEPSUN * EPSUNW)

EPS - dispersion of gaussian error cone

BET - Kuiper sunshape parameter beta

EPSUNW - 0.0046525 radian half-angle for sun. Parameter set in
DATA1

FEPSUN - Group 2 input factor to adjust solar width

JSUNA - index set to 1 when JSUN input as 8 to indicate that the
sunshape is represented by a single gaussian with rms
width consistent with the current insolation

/SUN/ Sun declination block

DECSM - maximum declination of sun
 FDEC - $2\pi/365.24$
 CDEC } cosine and sine of solar declination
 SDEC }

HS - local hour angle for sun
 DAY - day-of-year being processed
 TI - solar time-of-day being processed
 DELTAS - declination of sun

/SUNAIM/ Solar aiming block

ISUNA - when NPOIT=-1 on input, all heliostats are aimed directly at the sun. This option has been used to estimate shadowing for a series of parabolic dishes. The ISUNA value indicates need for this aiming

/SUNTAB/ Sunshape tabulation block

NTABL - number of values in XTL,YTL arrays
 XTL } arrays of observation-angle tangents and corresponding
 YTL } intensity of solar disk. These arrays are part of Group 2
 input when JSUN=7

/SUN2/ Error-cone transformation block

ECXSC } elliptic-normal error-cone parameter used when ICON > 3
 ECYSC } and when a new effective sunshape is to be evaluated
 ECASC }

ECXRR } in PHI the routine ENORM is called to convert the first
 ECYRR } three variables (in the sun-concentrator reference system)
 ECARR } to the corresponding last three variables in the
 reflected-ray reference system

/TABLE/ One-dimensional numerical convolution sunshape block

NTABLE - number of tabular entries giving sunshape when 1-D sunshape is used with numerical convolution for effective sunshape (17)
 NDIV - set to 4 in INDATA. NTABLE=2 ** NDIV + 1 also in INDATA. Parameter is also used in FI function
 XT } array of tangents of observation angles and corresponding
 YT } intensity for effective sunshape
 INTERP - index for interpolation method within XT,YT arrays. This is a Group 2 input parameter

Common Block

Parameter List

EL - cutoff value for tangent of observation angle when effective sunshape evaluated by 1-D numerical convolution

/TARGET/ Target block

XEXT - horizontal extent (m or radians) of target
 ZEXT - vertical extent (m or radians) of target
 XTAR }
 YTAR } three coordinates for target center when ITAR > 0
 ZTAR }

ITAR - index controlling input method for target center
 IGEO - index for detail desired in flux density information
 VTAR - array specifying target center and orientation. After input, these vectors are converted to three unit vectors along axes in the target coordinate system
 IVMD - index for direction of target normal

/TARXY/ Target mesh block

DX } horizontal and vertical distances between target points
 DZ }

MIDR - index for center row of target points
 MIDC - index for center column of target points

/TIM/ External sun position block

ELEVA } solar elevation and azimuthal angles when directly input to
 AZIMU } HELIOS

/TIMED/ Shadowing and blocking time block

NDYEAR - day-of-year being processed
 TIMD - time-of-day being processed

/TRITST/ Facet index identifier block

NFTEST - index for facet being processed

/TRKER/ Two-dimensional sunshape block

NER - concentrator error index
 TH } array of elliptic-normal error-cone parameters for each
 SIGX } concentrator error treated
 SIGY }

NTR - tracking-error index
 TRH } standard deviation of aiming precision along
 TRV } horizontal and vertical tracking axes

Common Block

Parameter List

IDIM - number of dimensions in effective sunshape
IANLYT - convolution-method index
ECA } convolution of all concentrator error cones yields these
ECX } parameters describing the elliptic-normal concentrator
ECY } error cone
DIMAX } parameters indicating need for new effective sunshape when
DEMAX } ICON=9
DAMAX }

/USER/ USERA parameter block

EPSQU - square of error-cone dispersion parameter EPSG

/WINSTO/ Reconcentrator index block

ISECT - target-section index
IRECP - number of reconcentrator sections
IREL - IRECP + 1

APPENDIX E
HELIOS Subroutine Connections

Routine	Subroutines and Functions Called Within the Routine					
A	AZELA	CPQR	DATA1	DECSUN	ELAZS	INDATA
	OUTP	SECOND	SQRT	APADJ	FPADJ	
ABSA	SQRT					
ABSORP						
ACRSB						
ADOTB						
AIM						
ANGL	ATAN2					
APADJ						
APERT	ABSA	ADOTB	APERTV			
APERTV	ABSA	ACRSB	ADOTB			
ATM						
AUTSUN						
AZELA	ANGL					
AZELB	ANGL	JITTER				
B	AZELB	NORF	SECOND	SHBL		
BASKET						
C	ABSA	ANGL	ADOTB	COORD	FACET	FMAX
	FVOT	GLOAD	NORF	POWERI	POWREC	PROP
	RARE	REF	SECOND	SAXB	TARGET	
CONE	FI	SMODN	STEP	SUN	USERA	USERB
CONEA	FI	SMODN	STEP	SUN	USERA	USERB
CONV	FF	FOURT	GG			
CONVU	ABSA	ADOTB	VNORT	ACRSB		
COORD						
CPQR	ANGL	FN	FVOT	MINA	SAXB	
CSHAPE						
D	CONEA	CONV	FF	FI	FIN	FR
	FZ	GG	GN	GR	NORM	QNC7
	SECOND	TONE				
DATA1	ATM	CONVU				
DECSUN	ATAN2					
ELAZS	ANGL	ATM	SRATIO			
ELNOR	ATAN2					
ELROT						

<u>Routine</u>	<u>Subroutines and Functions Called Within the Routine</u>				
ENORM					
ERRCHK	ERRGET	ERRPRT	ERXSET		
ERRGET	ERSTGT				
ERRPRT					
ERSTGT					
ERXSET	ERSTGT				
FACET	APERT	BASKET	PHI	ROTZ	RVN
	TCIRP	VALRL3	VECCT		
FACETA	PHID	ROTZ	RVN	VALRL3	
FF	CONEA				
FFONE	CONE				
FI					
FIN	FI				
FMAX					
FN	FACETA				
FOUR	SECOND				
FOURT	ERRCHK	MLUSED			
FPADJ	APADJ				
FR	FF				
FRES	INTRP1				
FU	VAL2D				
FV	FU	GAUSS			
FVOT	ADOTB				
FZ	FF				
GAUSS	ERRCHK	FUN	ONECHK		
GETNSF	ABSA	ACRSB	ROTAT		
GG	CONEA				
GLOAD	ABSA	ACRSB	ATAN2	GETNSF	
GN	GG				
GR	GG				
HELIOS	AUTSUN	DECSUN	ELAZS	OVERLAY	RANSET
INDATA	ABSA	CONVU	ELNOR	ORTAR	
	RVN	SUNPAR	TARGET	VALRL3	
INTRP1					
INTRVL					
JITTER	ANGL	ATAN2			
MASON					
MINA	ERRCHK	FN	MLUSED		
MLUSED					
NORF					
NORM	F	QNC7			
NORMC	F	QNC7			
NUCONV	ELROT	FFONE	FOURT		
ONECHK	ERRGET	ERRPRT	ERXSET		
ORTAR	ABSA				
OUTP					

<u>Routine</u>	<u>Subroutines and Functions Called Within the Routine</u>					
OVER	MASON					
OVERLP	MASON					
PHI	ABSA	ABSORP	ACRSB	ADOTB	CONE	CSHAPE
	ELNOR	ELROT	ENORM	ERF	FRES	FV
	INTRP1	NORMC	NUCONV	QNC7	VALRL3	VAL2D
PHID	ABSA	ADOTB	FVOT			
PLATE						
POWERI						
POWREC						
PROP						
QNC7	ERRCHK	FUN	MLUSED	ONECHK		
RARE						
REF						
RFBS	ERRCHK					
RLUD	ERRCHK					
ROTAT	ABSA					
ROTZ						
RVN	PLATE	USERVN				
SAXB	ERRCHK	MLUSED	RFBS	RLUD		
SHBL	ABSA	ANGL	EOF	OVER	OVERLP	
SMODN	STEP					
SRATIO						
STEP						
SUN						
SUNPAR						
TARGET	ABSA	ADOTB	AIM	USERTG		
TCIRP	ABSA	ADOTB				
ZONE	CONEA					
USERA						
USERB						
USERTG	ATAN2					
USERVN						
VALRL3						
VAL2D	ERRCHK	INTRVL				
VECCT						
VNORT						

<u>Routine</u>	<u>Subroutines and Functions Calling Routine</u>					
ABSA	APERT	APERTV	C	CONVU	GETNSF	GLOAD
	INDATA	ORTAR	PHI	PHID	ROTAT	SHBL
	TARGET	TCIRP				
ABSORP	PHI					
ACRSB	APERTV	CONVU	GETNSF	GLOAD	PHI	

<u>Routine</u>	<u>Subroutines and Functions Calling Routine</u>					
ADOTB	APERT PHID	APERTV TARGET	C TCIRP	CONVU	FVOT	PHI
AIM	TARGET					
ANGL	AZELA	AZELB	CPQR	ELAZS	JITTER	SHBL
APADJ	C	A	FPADJ			
APERT	FACET					
APERTV	APERT					
ATM	DATA1	ELAZS				
AUTSUN	HELIOS					
AZELA	A					
AZELB	B					
BASKET	FACET					
CONE	FFONE	PHI				
CONEA	D	FF	GG	TONE		
CONV	D					
CONVU	DATA1	INDATA				
COORD	C					
CPQR	A					
CSHAPE	PHI					
DATA1	A					
DECSUN	A	HELIOS				
ELAZS	A	HELIOS				
ELNOR	INDATA	PHI				
ELROT	NUCONV	PHI				
ENORM	PHI					
ERF	PHI					
ERRCHK	FOURT SAXB	GAUS8 VAL2D	MINA	QNC7	RFBS	RLUD
ERRGET	ERRCHK	ONECHK				
ERRPRT	ERRCHK	ONECHK				
ERSTGT	ERRGET	ERXSET				
ERXSET	ERRCHK	ONECHK				
F	NORM	NORMC				
FACET	C					
FACETA	FN					
FF	CONV	D	FR	FZ		
FFONE	NUCONV					
FI	CONE	CONEA	D	FIN		
FIN	D					
FMAX	C					
FN	CPQR	MINA				
FOURT	CONV	NUCONV				
FPADJ	A					
FR	D					
FRES	PHI					
FU	FV					

<u>Routine</u>	<u>Subroutines and Functions Calling Routine</u>					
FUN	QNC7	GAUS8				
FV	PHI					
FVOT	C	CPQR	PHID			
FZ	D					
GAUS8	FV					
GETNSF	GLOAD					
GG	CONV	D	GN	GR		
GLOAD	C					
GN	D					
GR	D					
INDATA	A					
INTRP1	FRES	PHI				
INTRVL	VAL2D					
JITTER	AZELB					
MASON	OVER	OVERLP				
MINA	CPQR					
MLUSED	FOURT	MINA	QNC7	SAXB		
NORF	B	C				
NORM	D					
NORMC	PHI					
NUCONV	PHI					
ONECHK	QNC7	GAUS8				
ORTAR	INDATA					
OUTP	A					
OVER	SHBL					
OVERLAY	HELIOS					
OVERLP	SHBL					
PHI	FACET					
PHID	FACETA					
PLATE	RVN					
POWERI	C					
POWREC	C					
PROP	C					
QNC7	D	NORM	NORMC	PHI		
RANSET	HELIOS					
RARE	C					
REF	C					
RFBS	SAXB					
RLUD	SAXB					
ROTAT	GETNSF					
ROTZ	FACET	FACETA				
RVN	FACET	FACETA	INDATA			
SAXB	C	CPQR				
SECOND	A	B	C	D	FOUR	
SHBL	B					
SMODN	CONE	CONEA				

<u>Routine</u>	<u>Subroutines and Functions Calling Routine</u>				
SRATIO	ELAZS				
STEP	CONE	CONEA	SMODN		
SUN	CONE	CONEA			
SUNPAR	INDATA				
TARGET	C	INDATA			
TCIRP	FACET				
STONE	D				
USERA	CONE	CONEA			
USERB	CONE	CONEA			
USERTG	TARGET				
USERVN	RVN				
VALRL3	FACET	FACETA	INDATA	PHI	
VAL2D	FU	PHI			
VECCT	FACET				
VNORT	CONVU				

APPENDIX F
File Names in HELIOS

The HELIOS computer code uses a series of files in processing a problem. The files are listed below to aid in adding further files, altering the recorded information, or using certain files for additional data processing.

<u>File Name</u>	<u>Used in Subroutine</u>	<u>Purpose</u>
Tape 1	GETNSF	Provides heliostat loading data (gravity, wind, . . .) for use in HELIOS.
Tape 2	A, C, INDATA	Stores data for separate heliostats. The tape is not used in HELIOS--external use only.
Tape 3	INDATA	Provides heliostat base coordinates when separate tape is more convenient than usual INDATA input. This file is used when IHELD=2.
Tape 4	B, C	Stores shadowing and blocking factors found in B for use in C when IHELD=2.
Tape 5	INDATA	Input.
Tape 6	Many Routines	Output.
Tape 8	CPQR	Punches prealignment data.
Tape 11	A	Stores heliostat data determined by prealignment and aim information.
	FOUR	Reads to calculate set of nearest neighbors.
	B	Reads to calculate heliostat alignment.
	C	Reads to update prealignment information.
Tape 12	SHBL	Temporarily stores blocking information.
Tape 14	B, C	B writes alignment data for use by C.

<u>File Name</u>	<u>Used in Subroutine</u>	<u>Purpose</u>
Tape 15	B	Stores alignment values for later use by B when lock occurs.
Tape 16	B	Stores new alignment values for each heliostat for later use by B when lock occurs.
Tape 22	SHBL	Combines blocking and shadowing information from Tapes 12 and 23 onto Tape 22.
	OVERLP, OVER	Temporarily stores shadowing or blocking data for one heliostat.
Tape 23	SHBL	Temporarily stores blocking or shadowing information.
	OVERLP, OVER	Combines shadowing and blocking data for each heliostat.
Tape 25	SHBL	Provides intermediate storage of blocking and shadowing for all heliostats at one time, for SHBL use.
Tape 40	A	Stores NDY,NTD,NHEST. A nonzero input parameter IPLOT1 should be 40 to identify the tape.
	C	Stores data for series of plot options.
Tape 41	FOUR	Stores set of nearest neighbors for each heliostat.
	OVER	Reads set of nearest neighbors.
Tape 43	C	Stores three-dimensional flux-density distribution data.
Tape 44	B, SHBL	Stores data for later reference for drawing shadowing and blocking diagrams.
Tape 45	D	Stores sunshape information for plotting.
Tape 49	C	Stores series of variables for shadowing and blocking diagram.
HELIOS	----	Contains all the overlays.
HELLGO	----	Resides on the SNLA NOS computer system only; this is the load-go file.

APPENDIX G
Jobstream Examples

7600 Execution From an Update File

The HELIOS Code and associated files reside on the permanent file system at SNL's computing center. Possible uses of such files are too numerous to illustrate, but some examples are given here to aid users in exercising various capabilities of the code. A typical CDC7600 jobstream that uses the HELIOS update file is illustrated below. This example includes plotting from both the PLO and PCTAR computer codes.

The HELIOS run cards:

```
JOB,MC7,...  
ACCOUNT,...,G4102,...  
FILE,OLDPL,RT=S.  
ATTACH,OLDPL,HELIOS.  
UPDATE,F.  
FTN,I=COMPILE,L=0,OPT=2.  
ATTACH,TAPE1,MMC-TAPE1-NASTRAN-SEPT79.  
    (for calculation including gravity loading effects).  
LDSET,PRESET=NGINF.  
MAP,OFF.  
LGO,PL=200000.
```

The plotting from PCTAR--3-D plots, contour plots, 90% power contours.

```
REWIND,TAPE43,TAPE44,TAPE45,LGO,COMPILE.  
UNLOAD,OLDPL.  
FILE,OLDPL,RT=S.  
ATTACH,OLDPL,PCTAR.  
UPDATE,F.  
FTN,I=COMPILE,L=0,OPT=2.
```

Attach DISSPLA plotting routines, driven by RSCORS.

```
ATTACH,DISSPLA,DISSPLA.  
ATTACH,RSCOR76.  
ATTACH,RSCDI76.  
LIBRARY,DISSPLA,RSCOR76,RSCDI76.  
LDSET,PRESET=NGINF.  
LGO.
```

Add the plots from PLO--sunshape plots, shadowing and blocking diagrams.

```
REWIND,LGO,COMPILE.  
FILE,OLDPL,RT=S.  
ATTACH,OLDPL,HELIOP.  
UPDATE,F.  
UNLOAD,OLDPL.  
FTN,I=COMPILE,OPT=2,L=0.  
LDSET,PRESET=NGINF.  
LGO.
```

Create plot file TEMP and copy BEMP from Tape 77.

```
ATTACH,POP,SCORPOP-7600,CY=1.  
POP,TAPE77,TEMP,FICHE.          IDENTIFYING COMMENT  
REWIND,TEMP.  
COPY,TEMP,BEMP.
```

Obtain hard copy of plot results.

```
LIBRARY,COMLIB.  
ATTACH,RHCNBP.  
BEGIN,RHC,RHCNBP,BEMP.
```

Obtain microfiche copy of printed output.

```
REWIND,OUTPUT.  
COPYCF,OUTPUT,FISH.  
FICHE,FISH.          IDENTIFYING COMMENT
```

Obtain microfiche copy of plot results.

```
COMQ,TEMP,DIC,FICHE,REV.
```

```
7/8/9    End of control deck  
         Update directives for HELIOS  
7/8/9    End of HELIOS update deck  
         HELIOS data cards  
7/8/9    End of HELIOS data  
         Update directives for PCTAR--should include proper dimension for  
         variables FZ, FM, XMAT, YMAT, and proper definition of NDIM.
```

NDIM is the number of target points along horizontal and vertical slices across the target.

FZ is dimensional NDIM,NDIM.

FM is dimensional NTARSH*11,NTARSH*11.

FZ is the array of flux densities at each of the 11-x-11 arrays of target points on the NTARSH**2 subtargets. The repeated edge

values are eliminated in forming FZ inside the code.
XMAT and YMAT are dimensioned NDIM and indicate target coordinates
of each target point.

7/8/9 End of PCTAR update cards
PCTAR data
7/8/9 End of PCTAR data
Update directives for PLO
7/8/9 End of PLO update
PLO data cards
7/8/9 End of PLO data
6/7/8/9 End of job.

If plotting of HELIOS results is to occur in a separate computer run, the
required tapes may be cataloged on the permanent file system and recalled later.
For example, PCTAR requires Tape 43. The control card

```
CATALOG,TAPE43,NAME,CN=...,RP=100.
```

catalogs Tape 43 under the name NAME, with a retention time of 100 days. The CN
is set equal to a code name the user assigns. Such data can also be saved on
personal magnetic tapes, as indicated below.

After the account card,

```
FILE,TAPE50,RT=S.  
STAGE,TAPE50,ST=MFA,HY,POST,VSN=personal tape number.
```

And after the first LGO card:

```
REWIND,TAPE43,TAPE44,TAPE45,TAPE50.  
RFL,30000.  
COPYBF,TAPE43,TAPE50,1.  
COPYBF,TAPE45,TAPE50,1.  
COPYBF,TAPE44,TAPE50,1.  
REDUCE.
```

Tapes 43, 44, and 45 are written by the HELIOS code. Tape 50 is the created tape
containing the data required for later plotting or further processing.

If a series of computer runs all use the same set of update cards, the
computer time required to compile the FORTRAN programs can be eliminated by using
binary files. However, we have found that changes are desired often enough that
binary files are not presently maintained. The FORTRAN compilation of HELIOS typ-
ically requires 23 s on the CDC7600; the typical time for a CRTF-222 heliostat run
is several hundred seconds.

Creation of a 6600 Binary File for HELIOS

Assume that an SNLA user has a series of problems with only a few heliostats. He might want to take advantage of the lower cost of the CDC6600 computer and its often faster (in clock time) return of results at SNLA to run his problems on the CDC6600. He would then want to create a binary file to save compilation time. The following jobstream will do the task.

```
JOB,MC6,...
ACCOUNT,...
ATTACH,OLDPL,HELIOS.
UPDATE,F,W.
FTN,I=COMPILE,L=0,B=HBIN,OPT=2.
COLLECT,HBIN,FTNLIB.
REQUEST,BB,*PF.
REWIND,HBIN.
COPY,HBIN,BB.
CATALOG,BB,HELIOSU-BINARY,RP=100,CN=...
7/8/9      End of control cards
7/8/9      End of HELIOS update directives
6/7/8/9    End of job.
```

CDC6600 Execution From the Binary File

```
JOB,CM130000,MC6,...
ACCOUNT,...,G4102,...
ATTACH,BIN,HELIOSU-BINARY.
PRESET,PIND.
MAP,OFF.
BIN,LC=200000.
7/8/9      End of control deck
              HELIOS data cards
7/8/9      End of HELIOS data
6/7/8/9    End of job.
```

With this deck a series of computer runs could be conveniently submitted to the computing system, and the often slight data changes could be made between runs.

Limitations

Examples in this appendix can only serve as models. Actual jobstreams are dependent upon the computer operating system currently in use and the acceptable control statements within that system. At SNLA the system has recently been converted from SCOPE 2.1 (CDC7600), SCOPE 3.3 (CDC6600), and NOS systems to a modified SCOPE 2.1 and an NOS operating system. At present these changes occur in the job, account, attach, catalog, and stage cards used above. A prospective user should contact his computing center for proper implementation.

APPENDIX H
HELIOS Code Summary

HELIOS purpose: The code was developed to evaluate designs for central-receiver, solar-energy-collector systems; to do safety calculations on the threat to personnel and to the facility itself; to determine how various input parameters alter the power collected; and to evaluate possible design trade-offs and individual heliostat performance.

HELIOS structure: The code, written in FORTRAN IV and designed with many subroutines for treating individual effects, has made needed additions and improvements easier as special requirements appeared. The additions also resulted in nonoptimum code design that will likely persist while effort is concentrated on more options. HELIOS has been divided into six overlays to reduce code-storage requirements.

Mathematical method: The method for evaluating flux density is basically the cone-optics approach. Reflector surfaces are divided into small segments treated as infinitesimal mirrors that reflect an effective solar image onto the target surface.

HELIOS input: Variables include atmospheric variables; sunshape parameters; coordinates for heliostat bases relative to the tower; heliostat design parameters, gravity-loading data, reflector and reconcentrator shape information; data describing the uncertainty resulting from surface errors, suntracking errors, nonspectral reflection, and wind loading; focusing and alignment strategy; aim point coordinates; receiver design; calculation time; parameters indicating effects to be included; and the chosen output options.

HELIOS output: Four options are available. The first gives the flux density (W/cm^2) produced by all the heliostats at the grid of target points. The power intercepted by the mirrors and that incident upon the target are given. The facet area reduced by the angle of incidence effect and the area further reduced by shadowing and blocking effects are given. These data are given for each designated calculation time.

The second output option yields the above output variables for each heliostat in addition to the total. The loss factor caused by light propagation between facet and receiver is also given for each heliostat.

The third output option is still more complete. It is especially useful for detailed examination of results for checking before a large computer

run. It includes facet and heliostat alignment information, sun orientation, target point alignment information, and detailed shadowing and blocking information including lists of the blocked (shadowed) and blocking (shadowing) heliostats.

All of the output options include (1) a table describing the built-in model of atmospheric mass as a function of apparent elevation angle of the sun; (2) a table describing the built-in model of atmospheric refraction as a function of solar elevation angle; (3) brief descriptions of the input data groups; (4) tabular distributions of the sunshape, the error cone, and the effective sunshape; (5) tower coordinates of each target point and the components of the unit vector normal to the target surface at each point in the grid; and (6) a listing of the main problem parameters. As a special output option, the three components of the energy flux density are available at each target point in the grid. Another option tabulates the angular distribution of the flux density at each target point.

The fourth output option is abbreviated and similar to the first, but in a form convenient for typewriter or NOS output.

Present HELIOS limitations:

- 1 \leq number of heliostats per cell \leq 559
- 1 \leq number of facets/heliostat \leq 25
- 1 \leq number of target points \leq 121
- 1 \leq number of prealignment points \leq 20
- 1 \leq number of aim points \leq 222
- 1 \leq number of reconcentrator surfaces \leq 6

Related Codes:

PLO - plotting program for shadowing and blocking diagrams, sunshape distribution, and a series of other possibilities. This code requires that computer software include DISSPLA.

PCTAR - plotting program for flux-density distribution at the target, contour-graphs of constant flux density, 3-D plots, evaluation of distribution centroid and of the contour containing 90% of the power incident upon the target. This code requires that computer software include DISSPLA. Both plotting codes are described in greater detail in Part IV of the user's guide.

Running time: The required running time is highly dependent upon input options. It is dominated by the flux-density calculation except at very late or early times when shadowing and blocking may be extensive. On CDC7600 with perfect-focus option, the flux-density calculation requires 14.4 ms/facet for 121 target points. Zones A-B and A-C-D-E (222 heliostats) of the CRTF require 11 to 18 s for shadowing and blocking calculations as those effects

reduce the effective mirror area by factors 0.99 to 0.81. Typical CDC7600 run time for 222 heliostats with 25 facets/heliostat and 121 target points is 120 s, including typical plotting. These times should be multiplied by $\leq n^2$ if the facets are divided into an n-x-n mesh for more precise integration.

Computer hardware requirements: HELIOS is operational on the SNL CDC6600 computer operating under Scope 3.3. The code requires 130K octal storage locations. HELIOS is also operational on the SNL CDC7600 and CYBER 76 under Scope 2.1.

Some auxiliary equipment is necessary.

Printer	- required
Microfiche output	- useful
Punch	- necessary for some options
Auxiliary storage	- necessary for recall of data temporarily on magnetic tape (disk)
Extended core storage	- necessary for tabulating angular distribution of flux density.

Computer software requirements: The coding language is FORTRAN Extended-Version 4. Required subroutines from the SNL library that are not distributed by the computer manufacturer are noted in Appendix III-A. These routines are included on HELIOS program tapes. The routines are summarized in Reference 3.

HELIOS status: The code is operational on CDC6600, CYBER 176, and CDC7600 computers. Versions of HELIOS have been converted for use on an AMDAHL computer at DFVLR in Stuttgart, Federal Republic of Germany, and for use on a UNIVAC computer at JPL, Pasadena, California. Its evolution is still in progress.

Developer/Sponsor:

C. N. Vittitoe	Central Receiver Systems Branch
F. Biggs	Division of Solar Energy
Theoretical Division 4231	Department of Energy
Sandia National Laboratories	Washington, DC 20545
Albuquerque, NM 87185	

Documentation: See References 1, 5, and 9. The present report completes the available documentation.

Availability: HELIOS is available from the authors.

Date: HELIOS became operational in April 1976. The present version of the code was formed in April 1981.

References

1. Frank Biggs and C. N. Vittitoe, The HELIOS Model for the Optical Behavior of Reflecting Solar Concentrators, SAND76-0347 (Albuquerque, NM: Sandia National Laboratories, March 1979).
2. M. Collares-Pereira and A. Rabl, "The Average Distribution of Solar Radiation--Correlations Between Diffuse and Hemispherical and Between Daily and Hourly Insolation Values," Solar Energy, 22(2):155 (1979).
3. K. H. Haskell and W. H. Vandevender, Brief Instructions for Using the Sandia Mathematical Subroutine Library (Version 8.0), SAND79-2382 (Albuquerque, NM: Sandia National Laboratories, November 1980).
4. G. A. Korn and T. M. Korn, Section 14.10-7 of Mathematical Handbook for Scientists and Engineers (New York: McGraw-Hill, 1968).
5. C. N. Vittitoe and F. Biggs, A User's Guide to HELIOS: A Computer Program for Modeling the Optical Behavior of Reflecting Solar Concentrators, Part I Introduction and Code Input (Albuquerque, NM: Sandia National Laboratories, August 1981).
6. D. S. Mason, "Determination of Areas and Volumes of Intersection of Zones in Old and New Grids," Appendix B in TOOREZ Lagrangian Rezoning Code, SLA-73-1057 (Albuquerque, NM: Sandia Laboratories, April 1974), by B. J. Thorne and B. B. Holdridge.
7. C. N. Vittitoe and F. Biggs, "Terrestrial Propagation Loss," Proceedings of the 1978 Annual Meeting of the American Section of the International Solar Energy Society, August 28-31, 1978, SAND78-1137C (Albuquerque, NM: Sandia Laboratories, April 26, 1978).
8. C. N. Vittitoe and F. Biggs, Sum-of-Gaussian Representation of Sunshape, SAND80-1637 (Albuquerque, NM: Sandia National Laboratories, September 1980).
9. C. N. Vittitoe, F. Biggs, and R. E. Lighthill, HELIOS: A Computer Program for Modeling the Solar Thermal Test Facility, A Users Guide, SAND76-0346 (Albuquerque, NM: Sandia Laboratories, March 1977, 2nd ed June 1977, 3rd ed October 1978).

DISTRIBUTION:

The Aerospace Corporation
Solar Thermal Projects
Energy Systems Group
P. O. Box 92957
Los Angeles, CA 90009
Attn: L. Katz, Director

Department of Energy
Solar Thermal Power Systems
Central Solar Energy Division
Washington, DC 20545
Attn: G. W. Braun, Assistant Director

Department of Energy
Large Solar Thermal Power Systems
Central Solar Energy Division
Washington, DC 20545
Attn: G. M. Kaplan, Acting Chief

Department of Energy
Solar Geothermal and Electric Energy
Energy Technology Division
Washington, DC 20545
Attn: H. H. Marvin, Deputy Program Director

GESER
Ecole Centrale des Arts et Manufactures
Grande Voie des Vignes
92290 Chatenay - Malabry
France
Attn: C. Ouannes

Department of Energy
Large Power Systems Branch
Central Power Systems Division
Washington, DC 20545
Attn: J. P. Zingesser

Department of Energy (3)
Solar Energy Division
San Francisco Operations Office
1333 Broadway, Wells Fargo Building
Oakland, CA 94612
Attn: J. A. Blasy, Director
R. W. Hughey, Deputy Div. Director
S. D. Elliott

Department of Energy STMPO
Suite 210
9650 Flair Park Drive
El Monte, CA 91731
Attn: R. N. Schweinberg

Electric Power Research Institute
3412 Hillview Avenue
P. O. Box 10412
Palo Alto, CA 94304
Attn: J. Bigger

NASA-Lewis Research Center
21000 Brookpark Road
Cleveland, OH 44135
Attn: B. Masica

Public Service of New Mexico
P. O. Box 2267
Albuquerque, NM 87103
Attn: J. Maddox

Indian Institute of Technology
Solar Energy Group
Centre of Energy Studies
Hauz Khas, New Delhi-110029, India
Attn: A. K. Seth

McDonnell Douglas Astronautics Co. (3)
5301 Bolsa
Huntington Beach, CA 92647
Attn: R. H. McFee
J. B. Blackman
J. R. Campbell

Swiss Federal Institute for Reactor Research
5303 Wurenlingen
Switzerland
Attn: P. Kesselring

Sanders Associates (2)
MER 12 1214
95 Canal Street
Nashua, NH 03060
Attn: S. B. Davis
N. McHugh

Belgonucleaire
Societe Anonyme
Rue de Champ de Mars 25
B -1050 Bruxelles
Belgium
Attn: J. P. Fabry, Ingenieur

DFVLR
Pfaffenwaldring 38
7000 Stuttgart 80
Federal Republic of Germany
Attn: K. J. Erhardt

DISTRIBUTION (cont):

INITEC
Padilla 17
Madrid-6
Spain

Attn: F. Delgado

Head of Energy and Thermal Control Dept. (2)

Construcciones Aeronauticas, S. A.

CASA Space Division

Rey Francisco, 4

Madrid-8 Apartado 193

Spain

Attn: A. Escarda

J. L. Hildalgo

Snamprogetti (2)

20097 S. Donato Milanese

Milano, Italy

Attn: A. D. Benedetti

C. Micheli

Indian Institute of Technology

Dept. of Physics

New Delhi-29, India

Attn: R. N. Singh

C. T. I. P. International

30 Rockefeller Plaza

New York, NY 10020

Attn: C. Mazzolini

Israel Institute of Technology

Faculty of Mechanical Engineering

Technion City, Haifa 32000

Israel

Attn: G. Grossman

Foster Wheeler Development Corp.

12 Peach Tree Hill Road

Livingston, NJ 07039

Attn: G. D. Gupta

Solar Energy Research Institute (4)

Resource Assessment Branch

1536 Cole Boulevard

Golden, CO 80401

Attn: R. Hulstrom

J. Williamson

B. Butler

K. Touryan

General Electric (2)

1 River Road, Building 23, Room 334

Schenectady, NY 12345

Attn: R. H. Horton

W. F. Knightly

General Electric (2)

1 River Road, Building 6, Room 329

Schenectady, NY 12345

Attn: S. Schwartz

T. Curinga

Georgia Institute of Technology (2)

Solar Energy & Materials Technology Div.

Engineering Experiment Station

Atlanta, GA 30322

Attn: C. T. Brown

P. Mackie

Black & Veatch (3)

P. O. Box 8405

Kansas City, MO 64114

Attn: M. Wolf

S. L. Levy

J. T. Davis

University of Houston

Solar Energy Laboratory

4800 Calhoun

Houston, TX 77004

Attn: Fred Lipps

L. Vant-Hull

Acurex Corporation (3)

Alternate Energy Division

Aerotherm Group

485 Clyde Avenue

Mountain View, CA 94042

Attn: P. Overly

D. Brink

D. R. McCullough

S. C. Plotkin & Associates

6451 W. 83rd Street

Los Angeles, CA 90045

Attn: W. H. Raser

Westinghouse Advanced Energy (6)

Systems Division

P. O. Box 10864

Pittsburgh, PA 15236

Attn: J. Day

D. Hofer

M. Lipner

W. Parker

W. Pierce

C. Silverstein

DISTRIBUTION (cont):

General Electric Company
Space Division
Room 7246 CC&F #7
P. O. Box 8555
Philadelphia, PA 19101
Attn: A. J. Poche

Jet Propulsion Laboratory (4)
4800 Oak Grove Drive
Pasadena, CA 91103
Attn: P. Poon, MS 506-328
K. C. Bordoloi, MS 506-328
V. Truscello, MS 502-201
I. Khan, MS 506-328

Martin Marietta (6)
P. O. Box 179
Denver, CO 80201
Attn: W. Hart, MS S0510
G. A. Roe, MS S0510
P. Norris, MS C0403
J. Montague, MS C0403
T. Oliver, MS S0403
B. Zuver, MS S8120

Dynatherm Corporation
One Industry Lane
Cockeysville, MD 21030
Attn: D. Wolfe

Gruman Energy Systems
4175 Veterans Memorial Highway
Ronkonkona, NY 11779
Attn: G. Yenatchi

Bechtel Corporation
P. O. Box 3965
San Francisco, CA 94119
Attn: R. L. Lessley, 301-3

University of Minnesota
Department of Electrical Engineering
139 Electrical Engineering
123 Church Street, SE
Minneapolis, MN 55455
Attn: M. Riaz

University of Louisville
Department of Electrical Engineering
Louisville, KY 40208
Attn: K. C. Bordoloi

F. A. Blake
7102 South Franklin Street
Littleton, CO 80122

Boeing Engineering and Construction (2)
P. O. Box 3707
Seattle, WA 98124
Attn: B. Beverly, MS 9A-47
E. J. Valley

Boeing Engineering and Construction
625 W. Andover Park
Tukwila, WA 98188
Attn: F. Mahony

Booz, Allen & Hamilton, Inc.
8801 E. Pleasant Valley Road
Cleveland, OH 44131
Attn: C. G. Howard

New Mexico State University
Dept. of Mechanical Engineering
P. O. Box 3450
Las Cruces, NM 81803
Attn: G.P. Mulholland

Airesearch Manufacturing Co. of California
Dept 38 Mail Stop T-40
2525 W. 190th Street
Torrance, CA 90509
Attn: T. S. Smith

University of Waterloo
Electrical Engineering Department
Waterloo, Ontario
Canada
Attn: L. Y. Wei

Ohio State University
Department of Mechanical Engineering
206 W. 18th Avenue
Columbus, OH 43210
Attn: T. Pettenski

Veda Inc.
Building D
400 North Mobil
Camarillo, CA 93010
Attn: R. V. Vener

Purdue University
Dept. of Mechanical Engineering
Lafayette, IN 47907
Attn: L. K. Matthews

University of Illinois
Department of General Engineering
117 Transportation Building
Urbana, IL 61801
Attn: O. Coskunoglu

DISTRIBUTION: (cont)

1521	J. L. Mortley	4723	R. R. Peters
1537	N. R. Keltner	4724	B. D. Shafer
1550	F. W. Neilson	5513	R. J. Gross
1556	E. A. Igel	5523	J. R. Koterak
4200	G. Yonas	8124	M. J. Fish
4210	J. B. Gerardo	8324	J. D. Hankins
4230	J. E. Powell	8331	P. L. Leary
4231	T. P. Wright	8334	R. Y. Lee
4231	F. Biggs	8430	R. C. Wayne
4231	R. E. Lighthill	8431	P. J. Eicker
4231	C. N. Vittitoe (25)	8450	C. S. Selvage
4240	G. W. Kuswa	8451	C. S. Selvage(Actg.)
4250	T. H. Martin	8451	T. D. Brumleve
4700	J. H. Scott	8451	C. J. Pignolet
4710	G. E. Brandvold	8452	A. C. Skinrood
4713	J. V. Otts	8452	D. L. Atwood
4713	D. L. King	8452	A. F. Baker
4713	W. K. Bell	8452	L. V. Griffith
4713	D. B. Davis	8452	C. L. Yang
4713	J. T. Holmes	8453	W. G. Wilson
4713	L. O. Seamons	8453	E. T. Cull
4713	M. C. Stoddard	8453	P. De Laquil
4716	J. F. Banas	8214	M. A. Pound
4716	R. W. Harrigan	3141	L. J. Erickson (5)
4716	G. W. Treadwell	3151	W. L. Garner (3)
4717	J. A. Leonard		For: DOE/TIC (Unlimited Release)
4717	E. L. Harley		DOE/TIC (25)
4721	J. C. Zimmerman		(C. H. Dalin 3154-3)
4723	T. A. Dellin		

